Acta Pharmaceutica Sinica B 2024;14(6):2428–2446

Chinese Pharmaceutical Association
Institute of Materia Medica, Chinese Academy of Medical Sciences

Acta Pharmaceutica Sinica B

www.elsevier.com/locate/apsb
www.sciencedirect.com

REVIEW

Enhanced optical imaging and fluorescent labeling for visualizing drug molecules within living organisms

Ting Sun[a,c,†], Huanxin Zhao[a,†], Luyao Hu[g], Xintian Shao[a,f], Zhiyuan Lu[a], Yuli Wang[h,i], Peixue Ling[c,d], Yubo Li[g,*], Kewu Zeng[a,e,*], Qixin Chen[a,b,*]

[a]*School of Pharmaceutical Sciences, National Key Laboratory of Advanced Drug Delivery System, Medical Science and Technology Innovation Center, Shandong First Medical University & Shandong Academy of Medical Sciences, Jinan 250062, China*
[b]*Departments of Diagnostic Radiology, Surgery, Chemical and Biomolecular Engineering, and Biomedical Engineering, Yong Loo Lin School of Medicine and College of Design and Engineering, National University of Singapore, Singapore 119074, Singapore*
[c]*Institute of Biochemical and Biotechnological Drugs, School of Pharmaceutical Sciences, Cheeloo College of Medicine, Shandong University, Jinan 250012, China*
[d]*Key Laboratory of Biopharmaceuticals, Postdoctoral Scientific Research Workstation, Shandong Academy of Pharmaceutical Science, Jinan 250098, China*
[e]*State Key Laboratory of Natural and Biomimetic Drugs, School of Pharmaceutical Sciences, Peking University, Beijing 100191, China*
[f]*School of Life Sciences, Science and Technology Innovation Center, Shandong First Medical University & Shandong Academy of Medical Sciences, Jinan 250062, China*
[g]*School of Chinese Materia Medica, Tianjin University of Traditional Chinese Medicine, Tianjin 301617, China*
[h]*Tianjin Pharmaceutical DA REN TANG Group Corporation Limited Traditional Chinese Pharmacy Research Institute, Tianjin 300457, China*
[i]*Key Laboratory of Systems Bioengineering (Ministry of Education), School of Chemistry Engineering and Technology, Tianjin University, Tianjin 300072, China*

Received 30 October 2023; received in revised form 7 January 2024; accepted 25 January 2024

*Corresponding authors.
E-mail addresses: yaowufenxi001@sina.com (Yubo Li), zkw@bjmu.edu.cn (Kewu Zeng), chenqixin@sdfmu.edu.cn (Qixin Chen).
[†]These authors made equal contributions to this work.
Peer review under the responsibility of Chinese Pharmaceutical Association and Institute of Materia Medica, Chinese Academy of Medical Sciences.

https://doi.org/10.1016/j.apsb.2024.01.018

KEY WORDS

Optical imaging;
Drug visualization;
Fluorophore labeling;
Therapeutics

Abstract The visualization of drugs in living systems has become key techniques in modern therapeutics. Recent advancements in optical imaging technologies and molecular design strategies have revolutionized drug visualization. At the subcellular level, super-resolution microscopy has allowed exploration of the molecular landscape within individual cells and the cellular response to drugs. Moving beyond subcellular imaging, researchers have integrated multiple modes, like optical near-infrared II imaging, to study the complex spatiotemporal interactions between drugs and their surroundings. By combining these visualization approaches, researchers gain supplementary information on physiological parameters, metabolic activity, and tissue composition, leading to a comprehensive understanding of drug behavior. This review focuses on cutting-edge technologies in drug visualization, particularly fluorescence imaging, and the main types of fluorescent molecules used. Additionally, we discuss current challenges and prospects in targeted drug research, emphasizing the importance of multidisciplinary cooperation in advancing drug visualization. With the integration of advanced imaging technology and molecular design, drug visualization has the potential to redefine our understanding of pharmacology, enabling the analysis of drug micro-dynamics in subcellular environments from new perspectives and deepening pharmacological research to the levels of the cell and organelles.

1. Introduction

Much progress has been made in the development of targeted drugs that interact with specifical molecular or organellar targets. Treatments based on these drugs benefit from high specificity and lower side effects as compared with those using traditional cytotoxic drugs and drugs with multiple targets[1,2]. While targeted drugs facilitate precision therapies and come with important clinical benefits, problems like the difficulty of drug discovery and target verification, as well as the long development cycle need to be addressed. Validating the mechanisms of drug−target interaction directly is a key step in the targeted drug development process[3]. Recently, surface plasmon resonance, drug affinity responsive target stability, cellular thermal shift assay, and other technologies have been used to investigate the target-engagement mechanism of small-molecule drugs[4,5]. However, it remains difficult to measure the cellular distribution of the targeted drugs and achieve real-time *in situ* detection and direct visualization analyses *in vivo*. Therefore, monitoring drug−target interactions is critical for determining the precise target of drugs and designing new targeted therapies.

The visualization of drugs *in situ* and the tracking of their movements throughout living systems thus have emerged as critical strategies in modern therapeutics, as these techniques offer valuable insights into pharmacokinetics and pharmacodynamics, especially in the realm of targeted drugs[6-8]. Recent years have witnessed remarkable advancements in the field of drug visualization, largely driven by breakthroughs in optical imaging technologies and innovative molecular design strategies.

In particular, fluorescence imaging has emerged as a powerful tool, in forms including fluorescence confocal microscopy, fluorescence lifetime imaging microscopy, two-photon imaging microscopy, super-resolution microscopy (SRM) and near-infrared II (NIR-II) live imaging systems. These tools allow for the real-time monitoring of drug distribution and localization within biological tissues[9-11]. These techniques provide high sensitivity and spatial resolution, making them indispensable techniques in drug visualization studies. These optical imaging techniques are particularly valuable for rapid and biocompatible observation of intracellular molecular−target interaction events and for non-invasively tracking living cells[12-14]. Additionally, when imaging probes are used in conjunction with SRM, the images can achieve nanometer and subcellular resolution, which will contribute to the further exploration of the mechanism of drug−target interaction[15,16]. For example, new organellar transport mechanisms leading to resistance to platinum drugs have been revealed by fluorescent labeling and SRM[17], and the time-dependent distribution behavior of fluorescent dextran in areas of contact between mitochondria and lysosomes has been identified in a similar manner[18]. Moreover, the development of near-infrared (NIR) fluorescence imaging, particularly NIR-II fluorescence imaging, has expanded the possibilities for non-invasive drug visualization, capitalizing on the reduced photon absorption, decreased tissue scattering and negligible tissue autofluorescence in this spectral range[19]. Compared with conventional fluorescence imaging approaches, fluorescent probes with longer emission wavelength (1000−1700 nm) in the NIR-II window provide higher resolution and achieve deeper penetration depths, which has shown broad and excellent prospects for drug tracking in living tissues[20,21]. For instance, Yang et al. developed a theranostic nanomedicine (AuNCs−Pt) possessing NIR-II imaging and glutathione-scavenging abilities to monitor platinum transportation and to achieve the effect of efficacy gains and reduced toxicity[22]. More recently, Wei et al. also designed a biodegradable NIR-II tandem polymer for 56MESS delivering, which could monitor the endocytosis of nanoparticles *via* NIR-II imaging in deep-tissue effectively and provide feedback on anti-tumor targeted treatment *via* apoptosis imaging[23].

In parallel with advances in optical imaging, molecular design strategies have evolved to facilitate drug visualization[24,25]. The engineering of drug molecules with optical labels is a key approach to enable their detection and quantification in complex biological environments. Drugs can be rendered visible by fluorophore labeling, allowing researchers to study their biodistribution and metabolism as well as their interactions with target or off-target sites of action. Relative to other tracking

techniques, such as the use of radiolabeled compounds or immunofluorescence, fluorescent labeling holds multiple advantages, including simpler operation, higher sensitivity, better reproducibility, more consistent membrane permeability, and the opportunity to perform real-time *in situ* detection, which has proven to be particularly useful in the study of targeted drugs[26-28]. Still, unlike highly selective antibody-based biologics, fluorescent molecules are prone to off-target effects, leading to side effects and potentially serious toxicity[29]. Furthermore, some fluorescent molecules themselves serve as targeted drugs that not only have optical activity but also are specifically targeted to achieve pharmacodynamic effects *in vivo*[30-32].

This review aims to provide a comprehensive overview of the cutting-edge techniques and approaches that have revolutionized drug visualization in therapeutics. First, we introduce the progress of fluorescence imaging techniques and their applications in drug visualization. Second, we review the three main types of fluorescent molecules in the field of drug visualization: fluorophore−drug conjugates, natural fluorescent derivatives and *de novo*-designed visual drugs. Finally, we conclude this paper by discussing current challenges and prospects for the use of fluorescent molecules in targeted drug research. In particular, we highlight here the importance of multidisciplinary collaborations among chemists, biologists, and imaging experts to overcome these challenges and advance drug visualization in therapeutics. The insights gained from these studies hold great promise for facilitating the optimization of drug development, improving treatment efficacy, and enhancing our understanding of the complex interactions between drugs and living systems.

2. Advanced fluorescence imaging technologies and analytical tools

The development of optical imaging techniques has allowed research into targeted drugs to be performed at a high resolution and to be monitored *in vivo* in real time[33-35]. In order to generate useful data for these applications, it is necessary to generate high-quality images at the subcellular, cellular, and animal scales and to employ advanced image quantification tools to process complex information.

2.1. Optical imaging on subcellular and cellular scales

Multiple strategies have been developed to trace drugs on very small scales. Here, we describe a variety of subcellular and cellular imaging microscopes and illustrate their applications for drug visualization (Fig. 1).

2.1.1. Wide-field microscopy

Wide-field imaging is the most fundamental microscopic imaging technology. During wide-field fluorescence imaging, the fluorescent light sources are incident on the objective lens *via* a falling illumination light path through the beam-splitting prism, and then specimens are excited to produce fluorescence, which is returned to the objective lens subsequently. Then the fluorescence is filtered by the dichroic mirrors to filter out fluorescence with target wavelengths and reaches the detector. Based on the imaging principle of this foundational technology, it features relatively simple operation, fast imaging speeds, and intuitive evaluation of cell distribution and morphology. This form of imaging has been used in multiple ways. For example, Chen et al. developed an automated high-content screening platform to collect time-lapse images and thus quantify the multidimensional responses of *Schistosoma mansoni* post-infective larvae to drug treatment[36].

However, in wide-field fluorescence imaging, the entire specimen is illuminated so that fluorescence generated at different focal plane locations is detected, resulting in a decrease in contrast, which limits the maximum imaging resolution and imaging depth and prevents more detailed observations of drug−molecule interactions at the subcellular level.

2.1.2. Fluorescence confocal microscopy

Confocal microscopy is designed to obtain high-clarity images with a horizontal resolution up to the diffraction limit by focusing its laser beam inside the specimen and using a pinhole to effectively block photons from out-of-focus regions from entering the detector[37]. The so-called confocal is that the emission light source point, the object point on the focal plane and the detector imaging point are focused together. In an optical system for confocal microscope, a continuous laser light source passes through a small aperture and converges on the specimens by a spectroscope. The irradiated sample excites fluorescence and converges to the detector. In this way, the excitation fluorescence generated on or under the objective imaging focal plane is not in confocal with the detector imaging point, so there is no imaging interference. Fluorescence confocal microscopes have been available for more than 30 years, and the convenience of operation and widespread availability of the technique ensures that it will continue to play a prominent role in biological imaging, especially with recent breakthroughs in the development of targeted drugs[38]. As it allows repeated imaging of the same area at different points in time, it is an excellent way to monitor disease progression and post-treatment response, and it is an effective way to explore the dynamics of targeted drugs in real time[39].

Compared with wide-field imaging, confocal imaging requires large image storage space and complex computer image processing technology by reconstructing the image obtained from multi-point scanning and then using the computer to complete the image display[40]. In addition, it is also limited by the diffraction limit, making it difficult to achieve super-resolution imaging at the subcellular level.

2.1.3. Two-photon microscopy

Tissue-penetrating techniques provide the potential to allow real-time observations of individual cells in intact living samples. In this regard, the penetrating ability of the photons that simultaneously excite the fluorophore in two-photon microscopy has led to the importance of this method in modern drug evaluation and oncology research[41,42]. Different from the direct irradiation of a continuous short wavelength laser in common confocal microscopy, two- or multi-photon microscopy excites specimens by using long wavelength photons, which have lower energy than short wavelength photons, that is, the sample needs to absorb two or more photons to achieve the energy generated by an equivalent short wavelength light source. This can reduce the damage to the specimen, making two-photon imaging gradually become powerful tools for the investigation of microspecies[43]. The technique does not require fixation or staining of biological tissues, which increases its capacity as a diagnostic tool. For instance, Li et al. found that multiphoton imaging can distinguish slight, significant, or complete tumor responses and can detect morphological alterations associated with the extracellular matrix during the progression of breast cancer[44]. In addition, because of its

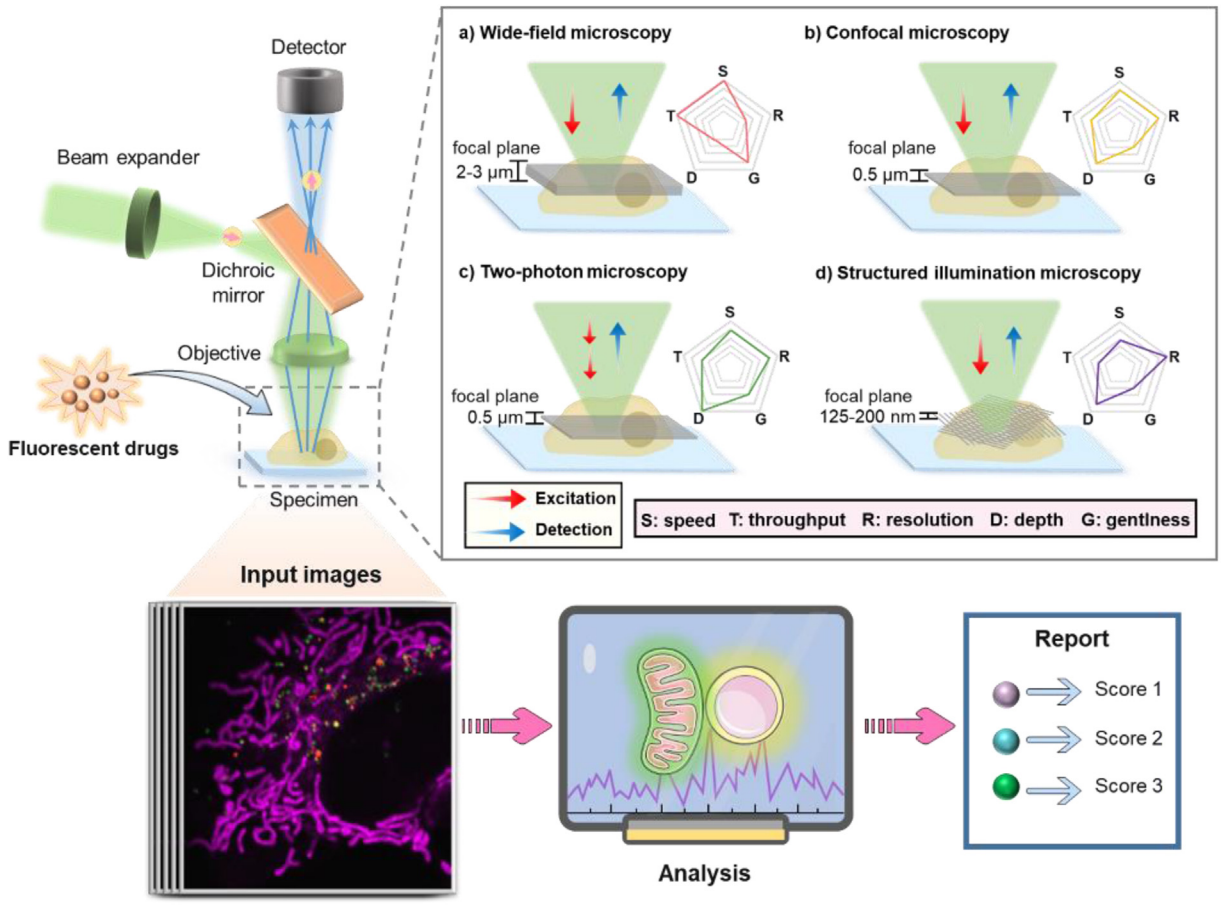

Figure 1 Principles underlying imaging-based technologies for drug visualization and screening.

ability to visualize protein activity with high spatiotemporal resolution in living cells within tissues, two-photon microscopy has been used to investigate signal transduction mechanisms, such as actin polymerization in hippocampal neuron synapses[45], astrocytic calcium signaling in the living murine brain[46], and multiplane calcium imaging of over 1000 neurons in mice[47].

Although two-photon imaging currently defines the upper limit of penetration depth in diffraction-limited microscopy, typical two-photon setups usually achieve worse resolution than that of confocal microscopes because the diffraction-limited focal spots widen as the illumination wavelength increases. Meanwhile, two-photon is also limited by the diffraction limit just like common confocal microscopy.

2.1.4. *Super-resolution microscopy*

The diffraction limit comes from the broadening of the imaging target, which is caused by the fluorescence emitted at different times being received and displayed by the detector. That is to say, if the diameter of the imaging spot can be made infinitely small, the diffraction limit will be broken[48]. All of the aforementioned microscopic imaging techniques are constrained by the diffraction limit, but recently developed SRM techniques, such as stimulated emission depletion (STED)[49], structured illumination microscopy (SIM)[50], and stochastic optical reconstruction microscopy (STORM)[51], change the imaging principle at the molecular level to overcome the diffraction limit and provide new tools for investigating interactions of drugs with organelles on the subcellular level. Work by Chen et al. has demonstrated the application of an innovative SIM approach to the study of biological activities of drugs, and in particular, they identified therapeutic interactions with mitophagy[15]. This work also revealed the occurrence of mitochondrion−lysosome interactions in living cells with improved accuracy. The application of SRM is also popular in other biological fields, including neurosciences[52,53], pathology[54], and cardiology[55].

However, the acquisition of high-resolution images takes a long time and requires pre-screening using a low-resolution microscope usually[56]. As its high resolution, SRM puts higher requirements on samples, optical Settings, and data processing. Therefore, these fluorescence imaging techniques should be combined according to the specific purpose of drug visualization in practice[57].

2.2. *Optical imaging at the whole-animal scale*

In contrast with *in vitro* and *ex vivo* imaging approaches, live animal imaging techniques allow the non-destructive capture of microstructural or functional images of biological tissues to evaluate treatment efficacy and disease development at the level of the whole animal[58-60]. Fluorescence imaging in the second near-infrared window (NIR-II, 1000−1700 nm) enables precise visualization of thick tissue features with a high signal-to-background ratio and high resolution due to minimal tissue scattering and low autofluorescence[61-63]. The most common optical detectors are

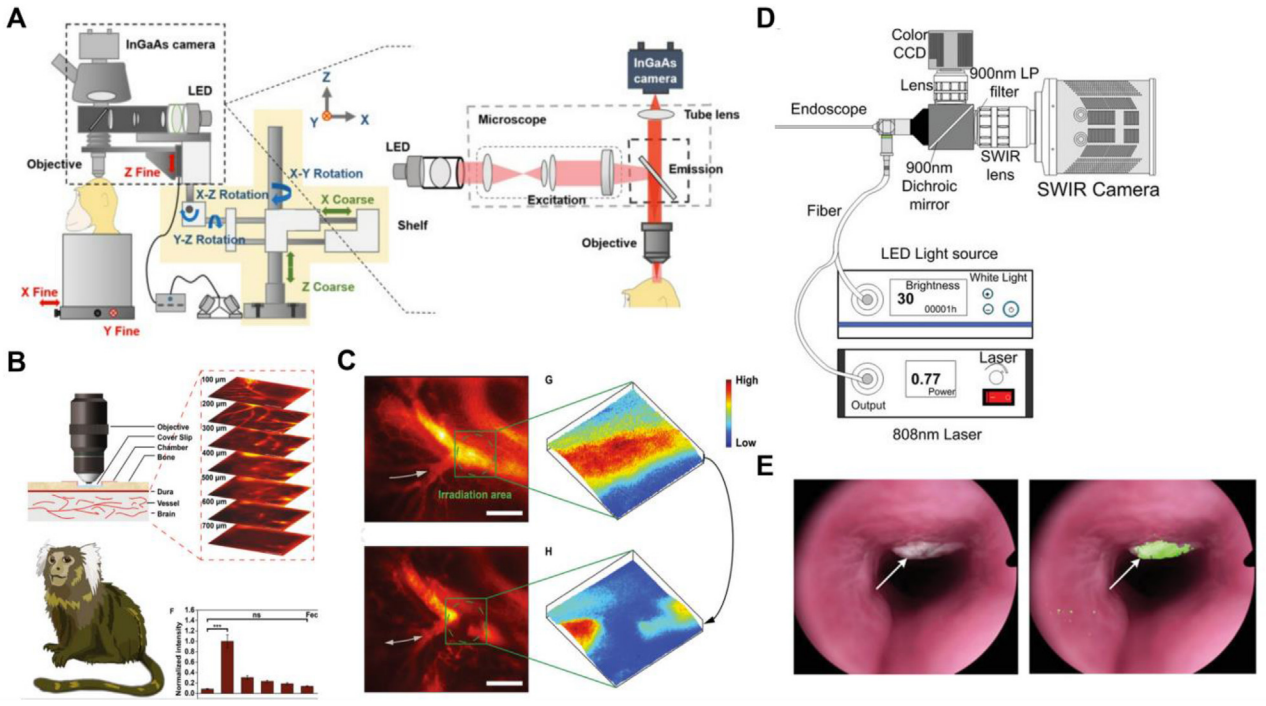

Figure 2 Application of NIR-II fluorescence microscopy. (A) Schematic illustration of the NIR-II fluorescence microscopic imaging system. Reprinted with the permission from Ref. 64. Copyright © 2020 The Authors, some rights reserved. (B) NIR-II fluorescence microscopy images of the cerebrovasculature through a thinned-skull window. (C) Distributions of 3D fluorescence intensity in brain blood vessels before and after induction of prothrombic ischemic stroke. Reprinted with the permission from Ref. 65. Copyright © 2021 Wiley-VCH GmbH. (D) Schematic diagram of the NIR-II endoscopy system. (E) Simultaneous white light and fluorescence images of representative tumors. Reprinted with the permission from Ref. 66. Copyright © 2019 WILEY-VCH Verlag GmbH & Co. KGaA, Weinheim.

silicon charge-coupled devices, which have detection ranges of 400−900 nm. Recently, newly developed semiconductor alloys, such as InGaAs, have overcome this limited range (Fig. 2A), allowing NIR-II fluorescence imaging to reach even higher sensitivity and resolution[64]. Techniques based on NIR-II have a relatively high penetration depth of approximately 2 cm, enabling it to allow researchers observe small blood vessels and identify signals emitted by deeper organs.

In order to validate the feasibility of NIR-II fluorescence imaging quality *in vivo*, Feng et al. utilized NIR-II fluorescence wide-field microscopy to investigate the cerebral vascular structure of marmosets[65]. The signals on each focal plane within nearly 800 μm below the thinned skull were almost completely captured upon axially modification of the relative position of the sample stage and the objective lens, and an ultrahigh spatial resolution of 2.4 μm was reached (Fig. 2B). Moreover, functional imaging in real time of the brain through the thinned skull was further conducted, and cerebrovascular alterations after brain embolism were observed (Fig. 2C).

Advanced NIR-II imaging also promises to provide doctors with an unparalleled view into tissues for tumor detection at greater depths and contrast[67]. For example, Suo et al. constructed a fluorescent endoscopic system that harnesses the power of the NIR-II fluorescence imaging window (Fig. 2D), and when the images from the fluorescent and visible channels were overlaid, data from this advanced endoscope provided intuitive and accurate delineation of colorectal tumor tissue in real time and permitted a more comprehensive understanding of disease progression (Fig. 2E)[66].

2.3. *Advanced image quantification tools*

The amount of data contained in high-resolution fluorescent images is becoming so large that tedious and subjective visual inspection is no longer sufficient. Instead, automated algorithms are being developed for the reliable and objective extraction of biological information from images acquired at the level of the cell or the organelle[68].

2.3.1. *Cell-based quantitative analysis*

CellProfiler software is the most notable tool for classifying and recognizing diverse cells, including tumor cells, human cells and Drosophila cells and for application to comet assays and other visual techniques that require high precision analyses[69,70]. Further, this software performs cell counting and scoring, yeast community classification, light correction, colocalization analysis, cell tracking, and more. For example, a novel method using CellProfiler was developed for the quantitative assessment of autophagy using images of cells expressing GFP-tagged WIPI1 acquired with confocal laser-scanning microscopy. As shown in Fig. 3A, this workflow can be quickly and easily adapted for the use of alternative autophagy markers or cell types, and it can also be used for high-throughput purposes[71].

2.3.2. *Organelle-based quantitative analyses*

The *M*-value system, based on full width at half maxima, was proposed in order to quantitatively analyze the crosstalk occurring at sites of mitochondria and lysosome contact (MLC) at the subcellular level[73,74]. This *M*-value provides an efficient platform

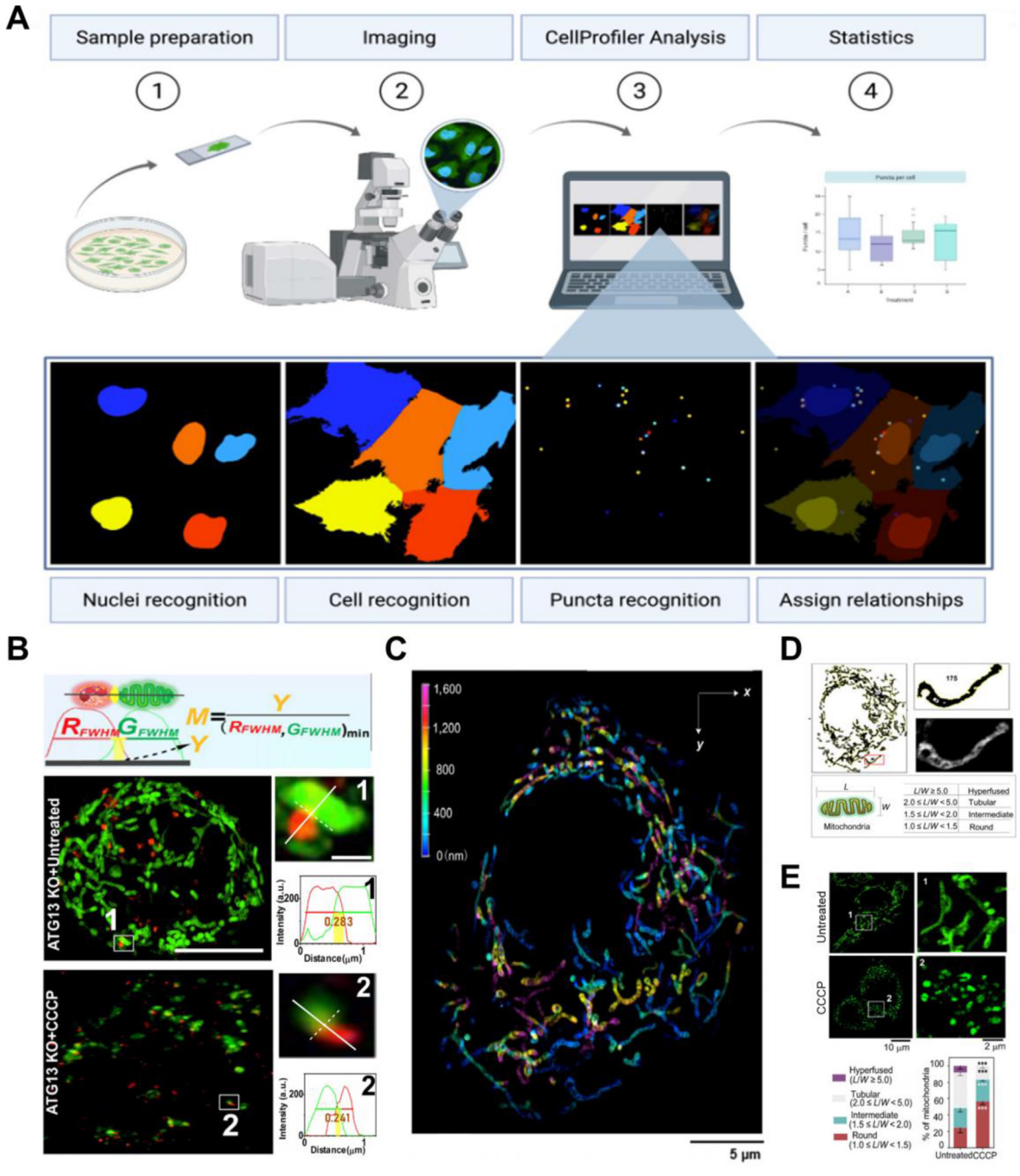

Figure 3 Advanced image quantification tools. (A) Procedure for fluorescence-based GFP-WIPI1 image acquisition and analysis using CellProfiler. Reprinted with the permission from Ref. 70. Copyright © 2023 The Authors, some rights reserved. (B) *M*-value calculations indicate mitochondria-lysosome contact events in ATG13KO cells (1,2) with or without treatment with the mitochondrial damaging agent. Reprinted with the permission from Ref. 72. Copyright © 2020 Elsevier Ltd. (C) Determination of the *L/W* value to evaluate changes to mitochondrial morphology in response to a drug. (D) Mitochondrial morphology of distribution parameters of *L/W*. (E) Use of the *L/W* value to evaluate mitochondrial morphological responses to CCCP treatment. Reprinted with the permission from Ref. 73. Copyright © 2020 Springer-Verlag GmbH Germany.

to quantify the interaction of subcellular organelles (Fig. 3B). Furthermore, a method of analysis of mitochondrial morphology (*L/W* value) in a single cell has been developed for accurately evaluating the mitochondrial response to drugs[72]. This method can quickly and accurately analyze the effects of small molecules and nano-materials on the distribution of mitochondrial morphologies in a single cell, enriching image analysis techniques for quantitative evaluation of drug-induced organellar damage (Fig. 3C−E).

2.3.3. *Organism-based 3D image analysis*

Currently, just a few analysis techniques have been developed for high-throughput 3D images, and the majority of image analysis

software is designed for 2D images[75]. 3D image analysis requires being flattened, *i.e.*, maximal projection, otherwise researchers need to develop particular programming to handle stereo structural data. Some open-source image analysis platforms, notably ImageJ and Fiji, are gaining popularity as they allow users to reconstruct plugins with more flexibility. Fiji can be employable to reconstruct three-dimensional images of *C. elegans* as well as to process long-term time-lapse images[76]. Di et al. developed an imageJ-based program for computing properties from the Z-stack maximum projection, that can efficiently analyze massive datasets to analyze F-actin morphology and branching patterns of breast cancer cell lines cultivated in spheroid culture[77]. In addition, a few commer cially available software packages include 3D-biological volumetric analysis platforms that are capable of evaluating enormous images obtained by high-throughput screening[77,78]. These software packages, however, are too expensive for smaller labs and do not allow for highly detailed images like 2D image analysis.

Because of these advances in imaging microscopy technology and high-throughput image analysis techniques, the evaluation of targeted drugs will move more quickly into the era of direct visualization *in vivo*[33,79,80]. Notably, this premise relies on the development of reliable fluorescent molecules capable of interacting with targets and providing information in the form of optical intensity. Therefore, we will next focus on the classification and design of fluorescent molecules for the assessment of targeted therapies.

3. Drug labeling strategies

3.1. Fluorophore−drug conjugates

Imaging-based quantitative molecular techniques are dependent on the development of precise fluorescent labeling technologies; in other words, both advanced imaging and labeling techniques are essential for the accurate evaluation of targeted drugs. Currently, visualization of small molecule drugs typically entails attaching fluorescent molecules to drug candidates. We list some recommended fluorophores, with excitation and emission wavelengths from the visible to the NIR-II window (Fig. 4)[81−84].

To date, in addition to small molecule probes, a variety of strategies for drug label tracing have been reported, including fluorescent quantum dots (QDs), upconversion luminescence, aggregates induced by emission (AIE) probes and so on. Among them, QDs are inorganic semiconductor nanocrystals, typically composed of a cadmium selenide (CdSe) core and a zinc sulphide (ZnS) shell and whose excitons (excited electron−hole pairs) are confined in all three dimensions, which gives rise to characteristic fluorescent properties[85]. As fluorescent probes, QDs are characterized by broad absorption profiles, high extinction coefficients, chemical stability and narrow and spectrally tunable emission profiles, which make QDs broadly used for biolabeling and bioimaging[86,87]. However, it is well known that QDs are excreted slowly, even for months, through the reticuloendothelial system, some of which become trapped for long periods, which may lead to long-term toxicity problems[88].

Upconversion luminescence is a kind of anti-Stokes shift luminescence, which breaks the traditional Stokes optical law. Its luminescence process refers to the luminescence process of emitting high-energy light (short wavelength) through a variety of conversion methods under the excitation of low-energy light (long wavelength). This optical imaging mode well solves the problems of biological spontaneous background light interference of fluorescent substances, low light penetration depth, and poor signal-to-noise ratio under Stokes law[89]. However, upconversion luminescence requires specific equipment, and the studied materials are mainly rare earth ion doped materials, which, like QDs, metabolize slowly, limiting its application in drug tracing[90].

Moreover, AIE probes have a unique luminescence characteristic. The molecular system does not emit fluorescence or weak fluorescence in the solution condition due to the free rotation of the chemical bonds. However, enhanced fluorescence is generated in the aggregation state because the rotation is inhibited. This phenomenon overcomes the aggregation-caused quenching effect of traditional fluorescent materials[91]. Researchers have designed many drug tracing methods based on AIE, but the triggering of AIE effect requires a high concentration of local molecules, reducing cytotoxicity is an urgent design consideration. At the same time, the ubiquitous conjugated phenolic rings in AIE probes may lead to intracellular distribution and metabolic problems[92].

Concretely speaking, small-molecule fluorescent probes have significant advantages in terms of the flexibility of fluorophores, which allows for the connection of various drugs to the function of image tracking. In addition, small molecules with good biodegradability, good biocompatibility and smaller size can be beneficial for absorbance and metabolism. Furthermore, small organic molecules are easy to synthesize, with good optical properties, strong fluorescence emission ability, and low preparation cost, and thus it is widely used in the imaging of small molecule drugs, which fits well with our goal of simultaneously visualizing drug distribution and studying the mechanism of action[93,94]. Therefore, we only focused on the small-molecule fluorescent probes for drug tracing in this review.

3.1.1. Critical components of fluorophore−drug conjugates

When conjugating drugs or biomolecules to fluorophores for evaluating drug−target binding in cells, tissues, and organs, the following factors need to be considered (Fig. 5).

3.1.1.1. Fluorescence quantum yield. A high fluorescence quantum yield is necessary for the visualization of a drug within a complex biological milieu[95,96]; therefore, the structure of the fluorophore−drug complex must be carefully considered to optimize fluorescence. In this regard, Fan et al. reported a fluorescent probe with a high quantum yield when conjugated to cisplatin[97]. Due to its high fluorescence quantum yield and two-photon absorption properties, this probe was able to detect cisplatin in cells and intact zebrafish, making this reagent a valuable tool.

3.1.1.2. Pharmaceutical activity. While adding multiple fluorophores would increase the sensitivity of live cell imaging, it is necessary to ensure that the fluorescently labeled group is inactive and that the activity of the drug molecule is not altered by the conjugation. Otherwise, the introduction of additional fluorophores may cause uncertainty about the pharmacological effect and may lead to conclusions that do not accurately reflect the true mechanism of action.

3.1.1.3. Stability. False positives will result if the bond between a fluorescent tag and a drug molecule is insufficiently stable[98]. Therefore, the reliable connection of fluorescent tags to the drug molecule is an important factor to be considered while designing fluorophore−drug conjugates[99]. The majority of coupling

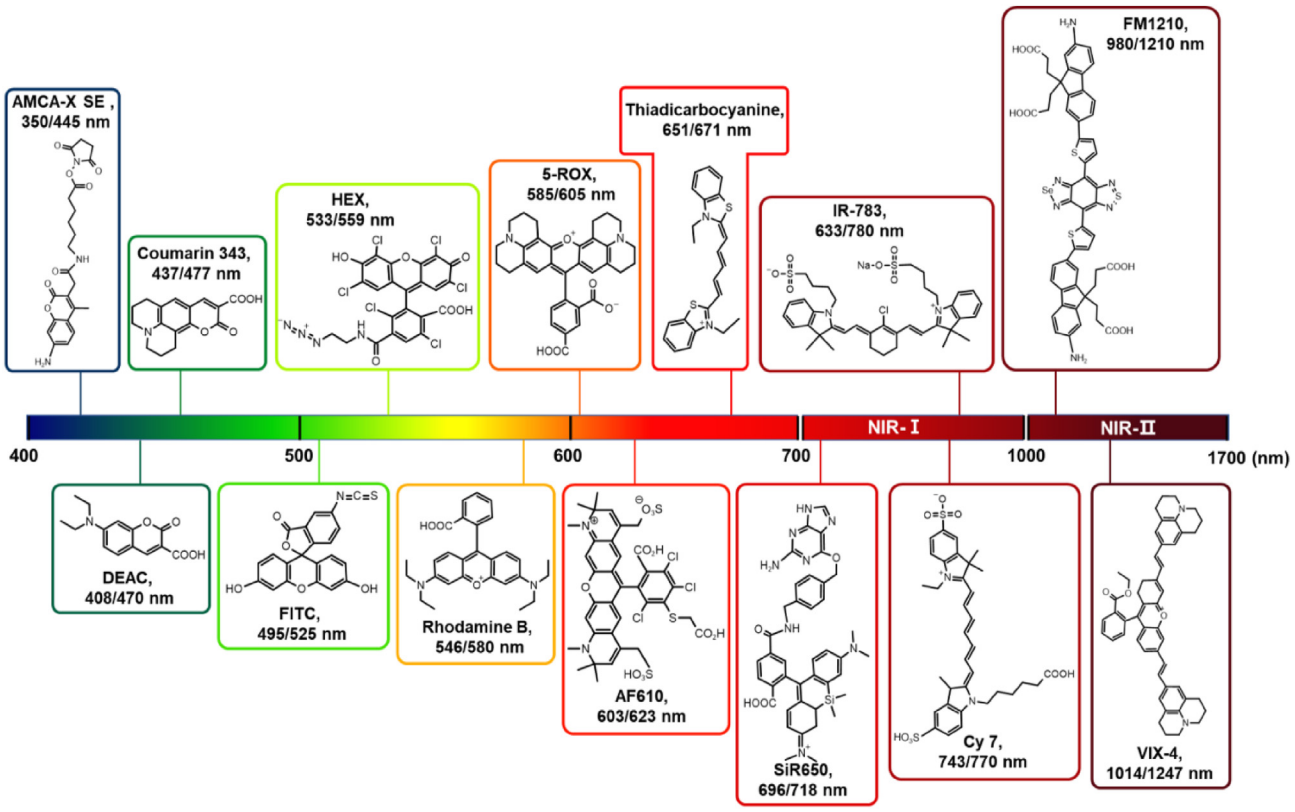

Figure 4 Recommend fluorophores from the visible window to near-infrared (NIR) II window.

techniques are based on ester amine or maleimide mercaptan bonds[100]. Wu et al. have investigated a mild coupling approach, the copper-catalyzed azide−alkyne cycloaddition reaction (CuAAC), and prepared a fluorescent glycoconjugate with good photophysical properties and effective cellular uptake[101].

A linker is commonly utilized to connect a fluorophore to a small bioactive molecule[102,103], and the structure of this linker can influence interactions between the two components. Ideally, the linker should be of moderate length and flexible enough to limit the independent rotation of the fluorophore without interfering with the binding of small active molecules to receptors. Moreover, identifying an appropriate attachment site that does not interfere with target binding is also critical. These factors are particularly important when studying antibiotics, which are usually relatively small molecules; the risk of chemical changes upon introduction of fluorophores is thus more severe[104].

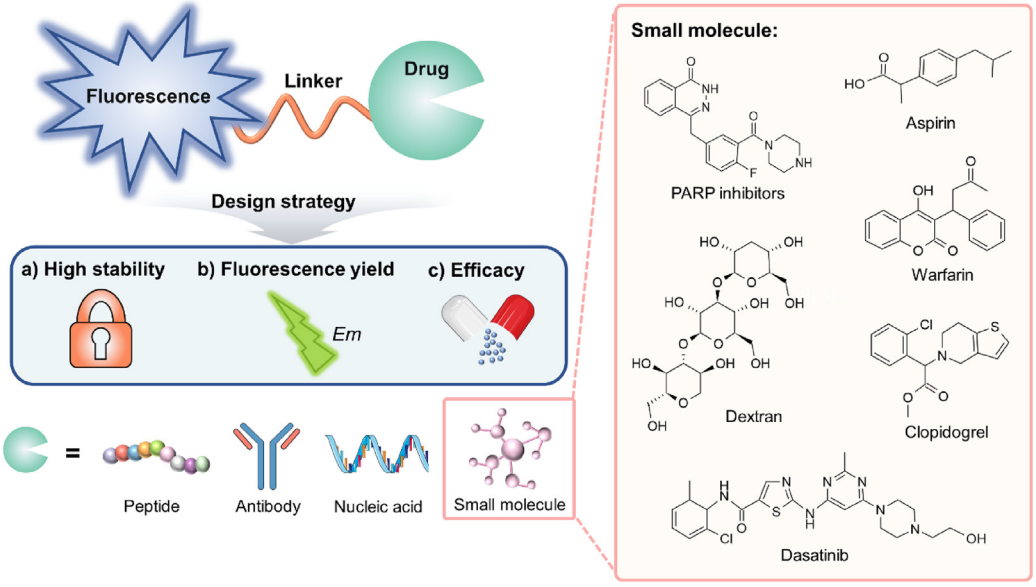

Figure 5 The main elements of directly fluorescently labeled drug technology for drug visualization.

3.1.2. *Application of the fluorophore−drug conjugates for drug tracking*

A targeted inhibitor of polyADP-ribose polymerase 1 (PARP-1) inhibitor, which slows DNA damage repair in rapidly proliferating cells, was the first anticancer drug approved for clinical application in combination with other anticancer drugs[105]. Thurber et al. described a strategy to visualize this inhibitor (PARPi) by conjugating it with small fluorophores to generate a drug that was both active for imaging and therapeutically active[83]. They used robust immobilization and cell tracking techniques in an *in vivo* investigation to perform intracellular pharmacokinetic imaging of PARPi in real-time, allowing them to record important early phases in the distribution of the drug.

More recently, Yue et al. designed a fluorescence-based strategy to analyze the roles of human serum albumin (HSA) in pharmacokinetics. They found that lysine-161 in HSA reacts specifically with a coumarin fluorescent dye, and this fluorescence was sensitive to interactions with HSA-binding drugs, including as ibuprofen, warfarin and clopidogrel[106]. The capability of the linked fluorescence probe to detect concentrations of drugs in the bloodstream was then demonstrated using ibuprofen as a model medication. Compared with traditional pharmacokinetic blood drug concentration monitoring methods, this non-invasive fluorescence imaging method was found to be more sensitive and to eliminate the need for continuous blood sample collection, which alleviates the pain of laboratory animals[107]. In addition to imaging diagnostic and monitoring, Kwon et al. designed a multifunctional fluorescent inhibitor to target prostate-specific membrane antigen (PSMA) and tumor hypoxia, using lysine as a scaffold to connect three different functional groups: a glutamate-urea-lysine (GUL) compound for inhibiting PSMA, 2-nitroimidazole to act as the hypoxia-sensitive moiety, and an NIR fluorophore for optical imaging (Fig. 6A)[108]. Consistent with the synergistic effects of the PSMA and hypoxic-targeting components, *in vivo* optical imaging and *in vitro* biological distribution analyses showed the accumulation of this multifunctional inhibitor at the tumor site (Fig. 6B).

At the subcellular targeting level, to realize the intracellular visual tracking of dextran, Chen et al. applied structured illumination microscopy (SIM) to capture the distribution of Cy5-labeled dextran (Fig. 6C). As shown in Fig. 6D, the intracellular transport of dextran from lysosome to mitochondria at different incubation times in living cells revealed the involvement of apoptosis and autophagy in the anti-tumor bioactivity of dextran[18]. Furthermore, Liu et al. designed a dinuclear platinum complex, Pt_2L, for tracking the behavior and distribution of platinum drugs in living cells[109]. Due to its super-large Stokes shift and excellent photophysical properties, they were able to track the photoactivated escape of Pt_2L from autolysosomes to the nucleus, where it attacked the DNA to specifically kill tumor cells (Fig. 6E). Since the autophagolysosome sequesters drugs, it provides additional avenues for the photoactivation of platinum drugs delivered as prodrugs to mitigate side effects.

Many additional fluorescently labeled small molecule drugs, antibodies[110,111], peptides[112], nucleic acids[113] and other molecules have been developed for the illumination and treatment of lesions[114]. However, the current visualization strategies based on fluorophore−molecule conjugates may lower drug efficacy, increase off-target effects, influence molecular interactions, and lead to other unpredictable effects, such as false positive results due to premature release of the fluorophore from the compound. Therefore, it is necessary to further improve fluorescence drug visualization strategies so that drug tracers may be monitored at the subcellular level and the mechanism of drug−target interactions can be validated.

3.2. *Natural label-free fluorescent derivatives*

Natural small molecules have a broad structural diversity, and many have intrinsic optical properties, which make them potentially superior to synthetic compounds with regard to biological relevance[115,116]. These natural compounds can be applied as optical probes or semi-synthetic optical probes to monitor physiological processes. Thus, fluorophores derived from plants, such as coumarins, flavonoids, alkaloids and curcumin, have attracted continuously increasing interest as an important source for the discovery and development of fluorescent targeted drugs (Fig. 7).

3.2.1. *Naturally derived visualization molecules*

Curcumin, the major yellow-orange diarylheptanoid pigment of *Curcuma longa*, possesses a great number of remarkable bioactivities, such as antitumor and anti-neurodegenerative activities[117]. Curcumin and its derivatives have been shown to decrease amyloid deposits *in vivo*, and they have been suggested as possible treatments for the neurodegenerative pathologies associated with Alzheimer's disease[118]. Because these compounds are naturally fluorescent, they are also being investigated as optical tracers of human amyloid deposits. Similarly, hypericin is a natural fluorescent photosensitizer (λ_{ex}: 570−590 nm, λ_{em}: 600−650 nm) found in some plants of the genus *Hypericum*. When this compound is administered to cancer patients, it accumulates in tumor tissues significantly more than it does in normal tissues, making it useful for photodynamic diagnosis (PDD) as a fluorescent marker for tumor detection and visualization[119]. As reviewed by Stone et al., some antibiotics have inherent fluorescence properties. The most widely investigated fluorescent antibiotics, such as mitomycin, chromomycin A3, and oligomycin, contain an anthraquinone core[120,121]. Other fluorescent natural small molecules with special pharmacological functions are shown in Table 1.

3.2.2. *Fluorophores targeting specific organelles*

While natural fluorophores are relatively abundant, few of them have specific intracellular targets or act as drugs that perform biological functions; especially rare are natural fluorophores that target specific organelles[133].

Recently, Wei et al. discovered a fluorescent molecule, magnoflorine, in a library of natural medicinal compounds[134]. Since the strong fluorescence of magnoflorine is revealed in response to hypochlorite (ClO^-) in the mitochondria, its distribution in subcellular organelles can be visualized by fluorescence imaging without additional labeling (Fig. 8A). Such experiments can be performed in parallel with classical experiments aimed at evaluating and quantitatively analyzing mitochondrial morphology[72]. As shown in Fig. 8B−C, MF and ClO^- engage in ferroptosis-specific reactions, suggesting that MF may be an interventional drug for the treatment of ferroptosis-related diseases, and it will also be an important tool for exploring the underlying mechanism of such diseases.

Many mitochondrial probes are designed to contain triphenylphosphonium (TPP), a lipophilic cation that can serve as a mitochondria-targeting flag in a variety of molecular contexts. For example, Denisov et al. designed a fluorescent probe containing a TPP moiety that accumulates in mitochondria and induces uncontrolled mitochondrial respiration (Fig. 8D)[135]. The brilliant fluorophore molecule also acts as a reporter of intracellular

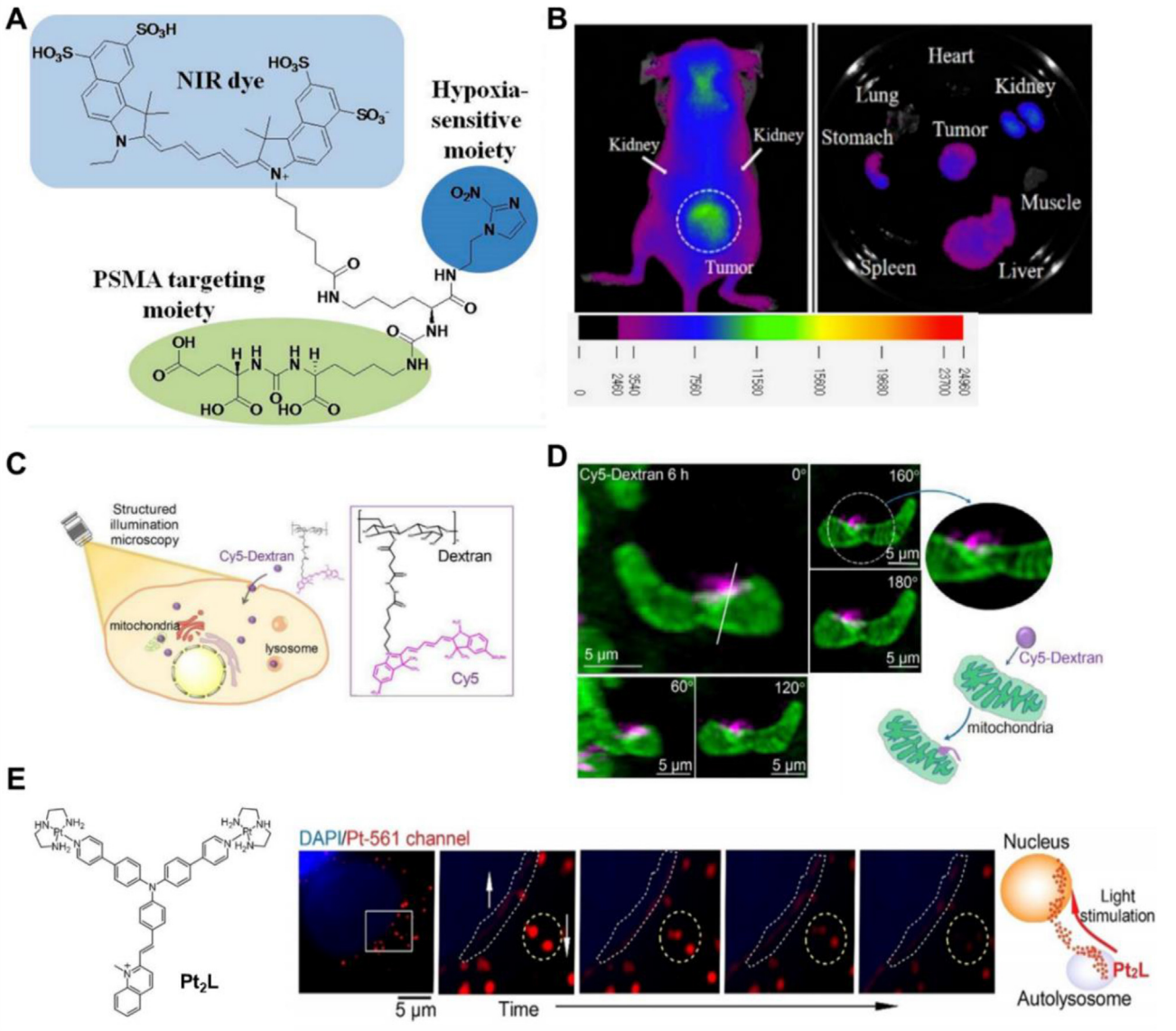

Figure 6 Direct fluorescent labeling for the visualizing of small molecule drugs. (A) The structure of a novel multifunctional prostate cancer-targeting fluorescent inhibitor. (B) *In vivo* targeting studies of novel multifunctional prostate-specific membrane antigen (PSMA) inhibitors. Reprinted with the permission from Ref. 108. Copyright © 2019 American Chemical Society. (C) Structured illumination microscopy-captured distribution of Cy5-labeled dextran. (D) Different angle images of the localization of Cy5-dextran to mitochondria. Reprinted with the permission from Ref. 18. Copyright © 2022 Elsevier B.V. (E) The dynamics process of photoactivated Pt_2L escaping from the autolysosomes to the nucleus. Reprinted with the permission from Ref. 109. Copyright © 2020 Wiley-VCH GmbH.

localization, and the targeted mitochondria uncoupler displays neuroprotective and nephroprotective capabilities.

The specific fluorescent derivatives that target organelles can be further modified to improve sensitivity and selectivity. However, the availability of fluorophores with specialized targeting or biological activity is currently limited[136], and the targeting action remains imprecise due to the complexity of the intracellular environment.

3.3. *High-throughput screening of fluorophores for visual drugs*

The specific targets of the majority of natural and synthetic fluorophores are uncertain[137,138]. Importantly, even small modifications in the structure of a fluorophore can influence its targeting. When the mechanism of recognition of a fluorophore for its target is unknown, the first stage in research is usually compound selection from a large pool of novel compounds[139].

3.3.1. *Process of fluorescent drug screening*

The discovery of visual drug is a challenging and exciting process that begins with the validation of biological targets and progresses through screening to narrow down potential molecules to identify prime candidates. Target confirmation of fluorescent drugs can be roughly classified into the type of target complexity: molecular, cellular, tissue slice, and live animals.

The initial screening of visual drugs is carried out by assessing the interactions between molecules that focus on interactions between candidate drugs and predicted targets, such as molecular

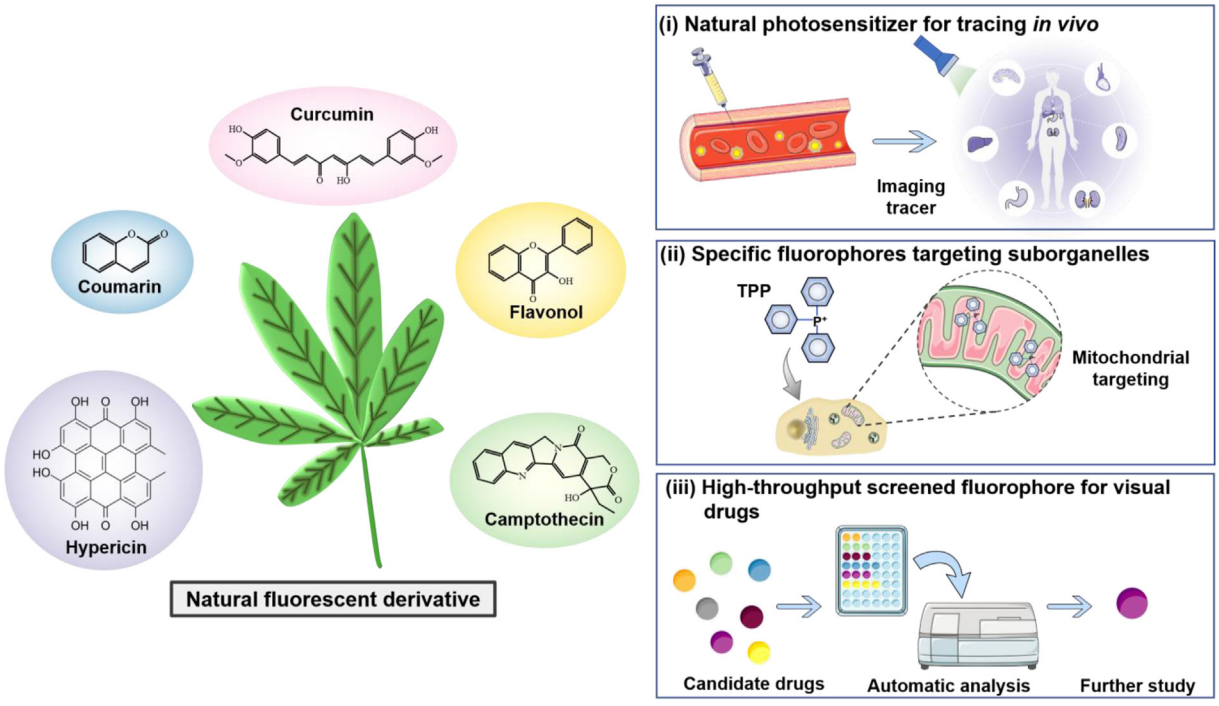

Figure 7 The types of natural label-free fluorescent derivatives for drug visualization.

docking[140], surface plasmon resonance (SPR)[141], microscale thermophoresis (MST)[142]. In a procedure known as high-throughput screening (HTS), these assays are designed to screen out hundreds of thousands of beneficial molecules from targeted libraries. As a next step, the selected compounds will next undergo to further cell-based screening. Despite the fact that cell studies were traditionally less suitable to HTS, technological advances in high-content screening (HCS) and integration of flow cytometry with plate readers have increased the use of high-throughput cellular assays for drug discovery[143]. Finally, the drug screening process was established by small mammals, which are highly similar to humans genetically as well as serve as a bridging stage between *in vitro* analysis and clinical studies. *In vivo* evaluation methods, in addition to classical non-imaging techniques such as LC−MS, due to advances in high-resolution imaging and image analysis tools, image-dependent techniques are also commonly applied to study biodistribution, pharmacokinetics, and biological activity of potential therapeutic agents, as well as to optimize drug delivery[144,145].

3.3.2. *Screening library of fluorescent molecules*

The diversity-oriented fluorescence library (DOFL), which is composed of thousands of small fluorescent molecules, and can be utilized to evaluate a wide variety of physiologically relevant targets systematically and objectively[146]. Various fluorescence imaging probes for drug discovery have been identified by combining DOFL with high-throughput unbiased screening. Lee et al. investigated the fluorescence response of a diversity-oriented BODIPY library (BD) by this screening strategy[147]. Based on the quantum yield changes in the presence of a variety of biomolecules, two novel fluorescent probes were discovered: BD-101 acted as a turn-on sensor for bovine serum albumin, while BD-187 demonstrated significant fluorescence quenching upon interaction with dopamine[148]. This high-throughput screening approach broadens the spectrum of targets available for drug visualization.

In addition, Zhu et al. established a program for screening a natural product database for the promising antimalarial drug target falciparum-2 (FP-2)[149]. Fluorometric tests were performed using Z-Leu-Arg-AMC as a substrate to rapidly evaluate the inhibitory activity of compounds in the natural product database against FP-2, and they found a new antimalarial lead compound, NP1024, an acylated flavonol oligosaccharide. Taking advantage of the fluorescence of NP1024, they found that NP1024 accumulated mainly in the food vacuole of the trophotrophoid parasite and bound to the target protein FP-2. The natural compound NP1024, as an inhibitor and fluorescent probe targeting FP-2, thus will provide a foundation for future research on integrating malaria diagnosis with treatment.

In short, a rising number of fluorescent derivatives with favorable target specificities and affinities have emerged, and these tools allow direct insight into target-selectivity, kinetics and pharmacological effects of drugs *in vitro* and *in vivo*. Nonetheless, the scale and diversity of the fluorescence probe library limit the success rate of this unbiased screening, and the hit rate needs to be improved in order to accelerate this work[150−152]. Moreover, due to the complicated structure and difficult synthesis of natural compounds, it is difficult to synthesize and construct enough fluorescent probes for screening. The design and synthesis of fluorescent molecular structures for specific targets will next be the focus of the visualization of targeted drugs.

3.4. *De novo-designed drugs for visualization*

Fluorescently labeled conjugates or fluorescent derivatives are associated with a series of challenges, such as off-target or false-positive fluorescence in cells and functional uncertainty of the target. However, pharmacophore-based drug design in the realm of precise treatments is even more demanding. Based on the strategy of *de novo* design, a series of bioactive and traceable molecules

Table 1 Fluorescent natural small molecules with pharmacological functions.

Fluorescent natural small molecule	Source	Emission (nm)	Pharmacological function
Camptothecin[122]	Camptotheca David	420	Anti-tumor
Coumarins[123,124]	Rutaceae and Umbelliferae	430–460	Anti-leukemia Anti-inflammation Anti-platelet aggregation Anti-tumor Immunomodulation
Quinine[125]	Cinchona Rubiaceae	450	Anti-malarial
Curcumin[126]	Turmeric	530	Anti-inflammatory Anti-oxidation Anti-proliferation Anti-angiogenesis
Cryptolepine[127]	*Cryptolepis sanguinolenta*	540	Anti-bacterial Anti-parasitic
Sanguinarine[128]	Papaveraceae Fumariaceae	568	Antibacterial Anti-inflammatory Cytostatic
Quaternary benzo[129]	Ranunculaceae Rutuaceae	560–600	Anti-bacterial Anti-fungal
Hypericin[130]	*Hyperforin perforatum*	600–650	Anti-viral Anti-depressant Anti-tumor
Fucoxanthin[131]	Brown algae and diatom	660–700	Anti-obesity Anti-diabetes Anti-neurodegenerative diseases
Siphonaxanthin[132]	Green algae and dinoflagellate	750	Anti-angiogenesis Anti-tumor

have been designed by fragment assembly[153], breaking through the limitations of known compounds and offering a broad unexplored chemical space for innovative drug discovery.

For instance, Lim et al. developed BD-tau, a BODIPY-based fluorescent probe that specifically detects pathological tau aggregates in live cells. Unlike other tau-selective probes, BD-tau is able to label tau aggregation induced by forskolin in live hippocampal neuronal cells[154]. As a cell-permeable imaging probe, BD-tau also selectively stains the tau aggregates in live brain tissues of tau transgenic mice, which will facilitate the

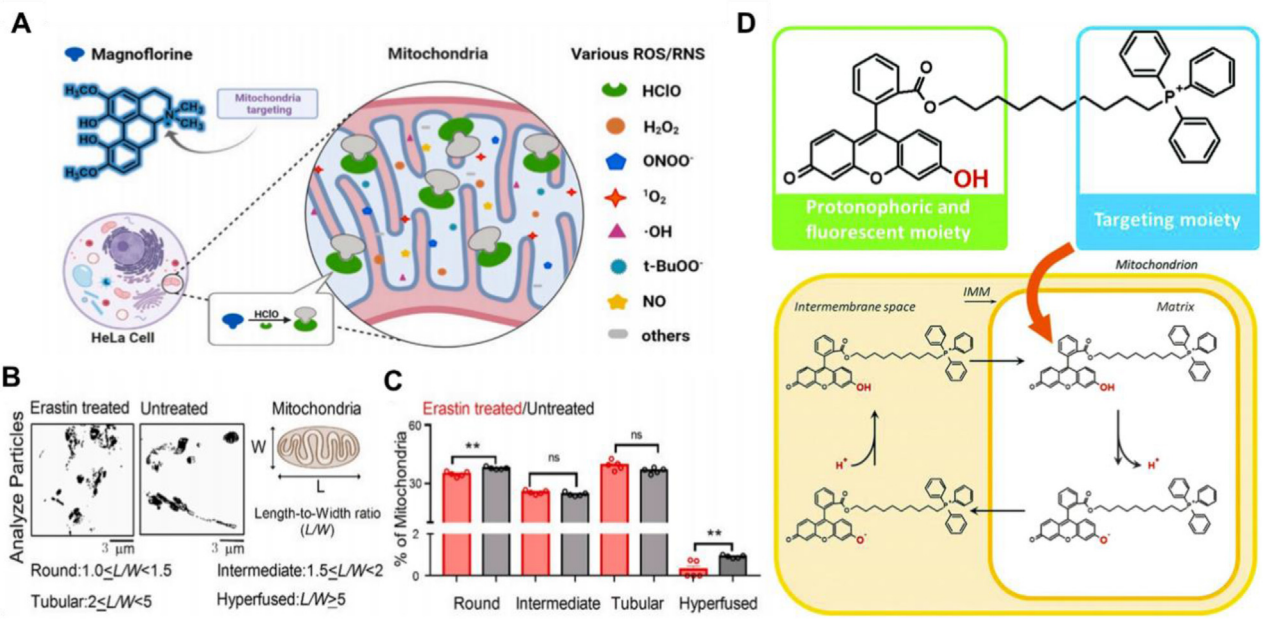

Figure 8 Specific fluorophores targeting organelles. (A) Schematic diagram of the responsiveness of magnoflorine to mitochondrial ClO^-. (B) Effect of MF on ferroptosis and the morphological distribution of mitochondria. (C) Quantitative analysis of mitochondrial morphology. Reproduced with permission. Data as shown as mean ± SD ($n = 5$). *$P < 0.05$, **$P < 0.01$, ***$P < 0.001$, all compared with untreated cells. Reprinted with the permission from Ref. 134. Copyright © 2022 Elsevier B.V. (D) Schematic representation of mitoFluo accumulation and uncoupling activity. Reprinted with the permission from Ref. 135. Copyright© 2014 Royal Society of Chemistry.

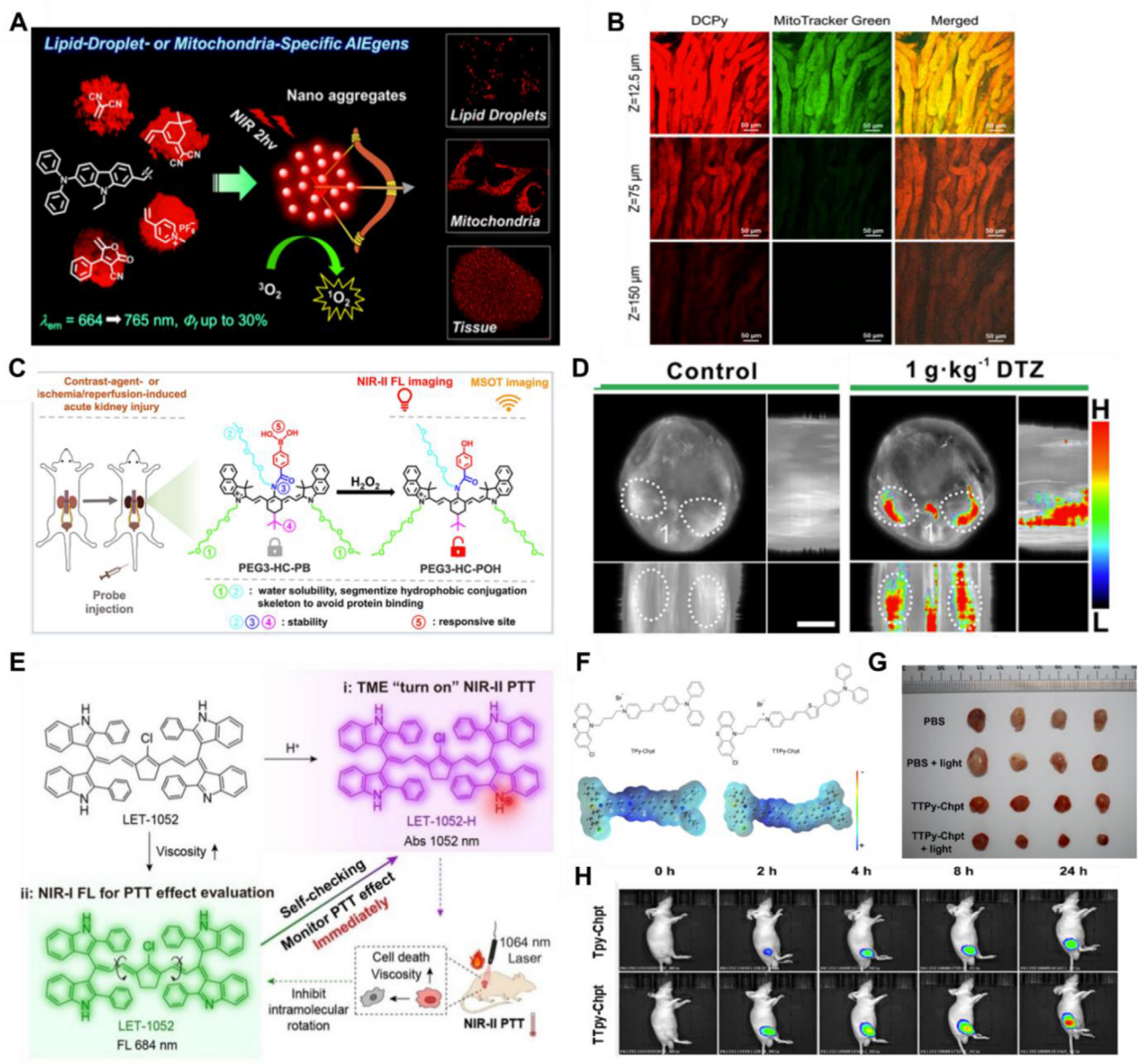

Figure 9 *De novo*-designed near-infrared probes for imaging therapeutics. (A) Schematic representation of organelle-specific photodynamic cancer therapy targeted to lipid droplets or mitochondria. (B) NIR AIEgens exhibit deeper tissue penetration than Mito-Tracker. Reprinted with the permission from Ref. 155. Copyright © 2018 American Chemical Society. (C) Design of NIR-II probes for noninvasive *in situ* detection of acute kidney injury (AKI). (D) 3D-MSOT images of control and AKI model mice at 5 h post-injection of the probe. Reprinted with the permission from Ref. 156. Copyright © 2023 American Chemical Society. (E) LET-1052 as a pH/viscosity-activatable molecule for acidic tumor microenvironment turn-on photothermal therapy. Reprinted with the permission from Ref. 156. Copyright © 2022 Wiley-VCH GmbH. (F) Chemical structure and surface electrostatic potential of TPy-Chpt and TTPy-Chpt. (G) Comparison images of tumors after PDT treatment. (H) Images of PC-3 tumor-bearing nude mice intratumorally injected with TPy-Chpt or TTPy-Chpt at different times. Reprinted with the permission from Ref. 157. Copyright © 2022 American Chemical Society.

investigation of tau pathology and the discovery of anti-tau-aggregate drugs.

To realize the visualization of deeper tissue *in situ*, a series of novel NIR fluorescent probes for biomedical imaging and diagnosis have been *de novo*-designed. In addition to high spatio-temporal resolution and deep tissue penetration, these probes can also specifically target subcellular organelles such as lipid droplets, mitochondria (Fig. 9A–B)[155]. Zeng et al. developed a high-performance NIR-II probe for noninvasive *in situ* detection and imaging of acute kidney injury (Fig. 9C)[156]. This probe is not designed to be therapeutic, but it was able to detect acute kidney injury induced by diatrizoate meglumine/diatrizoate sodium treatment of mice. This detection strategy utilizes real-time 3D-MSOT imaging upon response of the fluorophore to increased levels of H_2O_2 in areas of renal damage (Fig. 9D).

In addition to the above diagnostic imaging, *de novo*-designed probes, particularly those with specific targeting capacities, have also led to significant gains in therapeutic applications. Li et al.

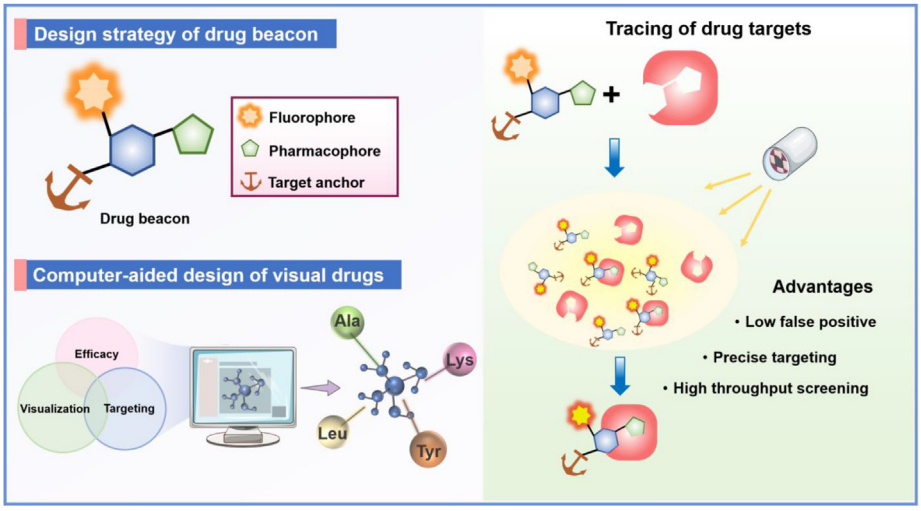

Figure 10 Schematic representation of the proposed design strategy for drug visualization.

designed LET-1052, a new molecule that is activatable by changes to pH and viscosity. As shown in Fig. 9E, the acidic tumor microenvironment can activate LET-1052, allowing it turn on NIR-II tumor bioimaging and photothermal therapy (PTT) under 1064 nm laser irradiation. Meanwhile, the efficacy of PTT may be monitored by instantaneous NIR-I tumor imaging of LET-1052 according to its viscosity-dependent response[158].

Zhang et al. synthesized two mitochondrial-targeting biological therapies, TPy-Chpt and TTPy-Chpt, through molecular functional design based on the traditional pharmaceutical raw material 2-chlorophenothiazine (Fig. 9F)[157]. Although they differ in mitochondrial targeting affinity, cellular imaging sensitivity, and cytotoxicity, they all have excellent *in vivo* and *in vitro* long-term NIR imaging and photodynamic therapy prospects. As shown in Fig. 9G−H, the NIR fluorescence signal is concentrated only on the tumor and does not spread to normal tissues, indicating that TPy-Chpt and TTPy-Chpt have some selectivity for tumor over healthy tissues, so the location of a tumor can be determined according to the position of fluorescence signal, facilitating tumor therapies.

The implementation of the *de novo*-designed strategy will unfold a new field for designing and visualizing targeted drugs, as well as a new direction for the identification of new targets and the study of lead compounds based on new functions within organelles. However, inadequate computational predictive power may result in poor biological relevance of the predicted structures, and synthesis methods are limited for the development of fluorophores with desirable optical and physicochemical properties, so the *de novo*-designed strategy needs to be enriched and modified for improved targeted drug visualization.

4. Conclusions and outlooks

In conclusion, the combination of advanced optical imaging techniques and innovative molecular design strategies has revolutionized drug visualization in therapeutics. Visualizing and monitoring drugs within living systems has great potential for optimizing drug development, enhancing treatment efficacy, and deepening our understanding of drug interactions within organisms. The continuous exploration of various fluorescent molecules and the development of multi-targeted and intelligent fluorescent molecules will undoubtedly drive further advancements in visible studies[159,160]. This review aims to promote the widespread application of fluorescent molecules and anticipates significant progress in the design and development of visualized drugs through the continuous advancement of optical imaging techniques and drug design procedures.

Previous studies have primarily focused on the use of fluorescent probes for tracing and detecting biomolecules, cells, and subcellular structures[161,162]. Recent advancements in technology have led to the design of various novel fluorescent molecules, including direct fluorophore−drug conjugates, fluorescein derivatives, and custom-designed molecules that combine fluorescence and pharmacodynamics. In this comprehensive review, we discuss the current trends in employing fluorescent-based probes for the development and design of targeted drugs. The discovery of several fluorescent targeted molecules has expanded the potential for precise disease diagnosis and treatment[163,164]. However, most targets identified for fluorescence derivatives have been uncovered through blind screening, resulting in a low success rate and unexpected outcomes. To enhance signal-to-noise ratios and enable dynamic imaging, reversible chemical selection and catalytic processes with signal amplification offer promising solutions, in contrast to the prevailing irreversible chemical connections[165−167]. Nonetheless, challenges such as off-target effects and false positives persist in the clinical application of fluorescent drugs. Despite these limitations, fluorescent drugs hold promise for diagnostics and disease treatment due to their direct visibility and real-time, high-resolution detection capabilities.

Moving forward, future research in drug visualization should focus on the following areas (Fig. 10):

(1) Proposing novel drug visualization design strategies, such as the integration of therapeutic, subcellular localization, and visualization capabilities into a single “drug beacon” molecule. The molecule that acts as a drug beacon needs to have the following three main functions, including (i) large conjugated fluorescence luminescence for advanced microscopy and imaging techniques, such as structured illumination microscopy (SIM); (ii) pharmacophore that is essential for biological activity; (iii) target anchor used as homing devices to guide drug beacons to specific organelles for efficacy. The strategy of “drug beacon” is of great

significance to trace the interactions between drugs and targets, and to elucidate the mechanisms of action of candidate drugs at the subcellular level.

(2) Encouraging the application of comprehensive technologies such as computer-aided drug design and the combination of various strategies including fluorescent drug design, super-resolution *in situ* tracers, ultrastructural analyses, algorithm development, and quantitative analyses.

(3) Fostering multi-disciplinary collaborations to address the clinical translation of drug visualization and leverage the expertise of experts from chemistry, biology, and molecular imaging. Currently, visualization drugs based on optical images of living organisms focus mainly on the aspects of surgical diagnosis, targeted therapy and therapeutic effectiveness assessment. Due to the complexity of the environment within the living organism, targeted delivery is often the most challenging. In order to the purpose of precision treatment, it is also necessary to design high-sensitivity, high-selectivity, diagnosis-synchronized "visual drugs" based on targeting and pharmacophore to further leverage in clinical applications.

Acknowledgments

This work was financially supported by the Shandong Province Key R&D Program (Major Technological Innovation Project, 2021CXGC010501, China), National Natural Science Foundation of China (Nos. 22107059, 22007060, 32300957, 82141209), Young Elite Scientists Sponsorship Program by CACM, China (CACM-2023-QNRC1-02), the key Program of Natural Science Foundation of Shandong Province (ZR2023ZD25, China), Natural Science Foundation of Shandong Province (ZR2021QH057, ZR2022QH304, ZR2020QB166, ZR2023QH427, China), Innovation Team of Shandong Higher School Youth Innovation Technology Program (2021KJ035, 2022KJ197, China), Taishan Scholars Project in Shandong Province, China (TSPD20181218; TSTP20230633; TSQN202211221), Shandong Science Fund for Excellent Young Scholars (ZR2022YQ66, China), Jinan New 20 Policies for Higher Education Funding (202228048, China), Natural Science Foundation of Shandong Province (Joint Fundation for Innovation and Development, ZR2022LZY021, China), Youth Qihuang Scholars Support Program of the State Administration of Traditional Chinese Medicine, Tianjin Graduate Research Innovation Project (General Project, 2022BKY180, China), TUTCM Graduate Research Innovation Project (General Project) and Shandong Province Traditional Chinese Medicine Science and Technology Project (M-2023208, China). We thank Translational Medicine Core Facility of Shandong University for consultation and instrument support.

Author contributions

Ting Sun, Huanxin Zhao, Luyao Hu, Xintian Shao, Zhiyuan Lu, Peixue Ling, Yuli Wang, Yubo Li, Qixin Chen, and Kewu Zeng conceived the project and wrote the manuscript.

Conflicts of interest

We declare that we have no financial or personal relationships with other people or organizations that can inappropriately influence our work.

References

1. Zhong L, Li Y, Xiong L, Wang W, Wu M, Yuan T, et al. Small molecules in targeted cancer therapy: advances, challenges, and future perspectives. *Signal Transduct Target Ther* 2021;**6**:201.
2. Zhao Z, Ukidve A, Kim J, Mitragotri S. Targeting strategies for tissue-specific drug delivery. *Cell* 2020;**181**:151−67.
3. Li T, Guo R, Zong Q, Ling G. Application of molecular docking in elaborating molecular mechanisms and interactions of supramolecular cyclodextrin. *Carbohydr Polym* 2022;**276**:118644.
4. Renaud JP, Chung CW, Danielson UH, Egner U, Hennig M, Hubbard RE, et al. Biophysics in drug discovery: impact, challenges and opportunities. *Nat Rev Drug Discov* 2016;**15**:679−98.
5. Prescher JA, Contag CH. Guided by the light: visualizing biomolecular processes in living animals with bioluminescence. *Curr Opin Chem Biol* 2010;**14**:80−9.
6. Licha K, Olbrich C. Optical imaging in drug discovery and diagnostic applications. *Adv Drug Deliv Rev* 2005;**57**:1087−108.
7. Choy G, Choyke P, Libutti SK. Current advances in molecular imaging: noninvasive *in vivo* bioluminescent and fluorescent optical imaging in cancer research. *Mol Imaging* 2003;**2**:303−12.
8. Blum G, von Degenfeld G, Merchant MJ, Blau HM, Bogyo M. Noninvasive optical imaging of cysteine protease activity using fluorescently quenched activity-based probes. *Nat Chem Biol* 2007;**3**:668−77.
9. Zhao W, Zhao S, Li L, Huang X, Xing S, Zhang Y, et al. Sparse deconvolution improves the resolution of live-cell super-resolution fluorescence microscopy. *Nat Biotechnol* 2022;**40**:606−17.
10. Qiao Q, Liu W, Zhang Y, Chen J, Wang G, Tao Y, et al. *In situ* real-time nanoscale resolution of structural evolution and dynamics of fluorescent self-assemblies by super-resolution imaging. *Angew Chem Int Ed Engl* 2022;**61**:e202208678.
11. Liu N, Chen X, Kimm MA, Stechele M, Chen X, Zhang Z, et al. *In vivo* optical molecular imaging of inflammation and immunity. *J Mol Med (Berl)* 2021;**99**:1385−98.
12. Shen J, Chen J, Wang D, Liu Z, Han G, Liu B, et al. Real-time quantification of nuclear RNA export using an intracellular relocation probe. *Chinese Chem Lett* 2022;**33**:4.
13. Edgington LE, Berger AB, Blum G, Albrow VE, Paulick MG, Lineberry N, et al. Noninvasive optical imaging of apoptosis by caspase-targeted activity-based probes. *Nat Med* 2009;**15**:967−73.
14. Ye Y, Chen X. Integrin targeting for tumor optical imaging. *Theranostics* 2011;**1**:102−26.
15. Chen Q, Fang H, Shao X, Tian Z, Geng S, Zhang Y, et al. A dual-labeling probe to track functional mitochondria-lysosome interactions in live cells. *Nat Commun* 2020;**11**:6290.
16. Yang Z, Samanta S, Yan W, Yu B, Qu J. Super-resolution microscopy for biological imaging. *Adv Exp Med Biol* 2021;**3233**:23−43.
17. Liu LY, Fang H, Chen Q, Chan MH, Ng M, Wang KN, et al. Multiple-color platinum complex with super-large Stokes shift for super-resolution imaging of autolysosome escape. *Angew Chem Int Ed Engl* 2020;**59**:19229−36.
18. Chen HM, Wang H, Wei YC, Hu MM, Dong B, Fang HB, et al. Super-resolution imaging reveals the subcellular distribution of dextran at the nanoscale in living cells. *Chinese Chem Lett* 2022;**33**:1865−9.
19. Becker A, Hessenius C, Licha K, Ebert B, Sukowski U, Semmler W, et al. Receptor-targeted optical imaging of tumors with near-infrared fluorescent ligands. *Nat Biotechnol* 2001;**19**:327−31.
20. Li C, Chen G, Zhang Y, Wu F, Wang Q. Advanced fluorescence imaging technology in the near-infrared-ii window for biomedical applications. *J Am Chem Soc* 2020;**142**:14789−804.
21. Chen G, Zhang Y, Li C, Huang D, Wang Q, Wang Q. Recent advances in tracking the transplanted stem cells using near-infrared fluorescent nanoprobes: turning from the first to the second near-infrared window. *Adv Healthc Mater* 2018;**7**:e1800497.
22. Yang Y, Yu Y, Chen H, Meng X, Ma W, Yu M, et al. Illuminating platinum transportation while maximizing therapeutic efficacy by

gold nanoclusters *via* simultaneous near-infrared-i/ii imaging and glutathione scavenging. *Acs Nano* 2020;**14**:13536−47.
23. Wei D, Yu Y, Huang Y, Jiang Y, Zhao Y, Nie Z, et al. A near-infrared-ii polymer with tandem fluorophores demonstrates superior biodegradability for simultaneous drug tracking and treatment efficacy feedback. *Acs Nano* 2021;**15**:5428−38.
24. Rudin M, Rausch M, Stoeckli M. Molecular imaging in drug discovery and development: potential and limitations of nonnuclear methods. *Mol Imaging Biol* 2005;**7**:5−13.
25. Stuker F, Ripoll J, Rudin M. Fluorescence molecular tomography: principles and potential for pharmaceutical research. *Pharmaceutics* 2011;**3**:229−74.
26. Zou Y, Li M, Xiong T, Zhao X, Du J, Fan J, et al. A single molecule drug targeting photosensitizer for enhanced breast cancer photothermal therapy. *Small* 2020;**16**:e1907677.
27. Zhang C, Shao H, Zhang J, Guo X, Liu Y, Song Z, et al. Long-term live-cell lipid droplet-targeted biosensor development for nanoscopic tracking of lipid droplet-mitochondria contact sites. *Theranostics* 2021;**11**:7767−78.
28. Wang H, Wang X, Li P, Dong M, Yao SQ, Tang B. Fluorescent probes for visualizing ROS-associated proteins in disease. *Chem Sci* 2021;**12**:11620−46.
29. Yang M, Baranov E, Jiang P, Sun FX, Li XM, Li L, et al. Whole-body optical imaging of green fluorescent protein-expressing tumors and metastases. *Proc Natl Acad Sci U S A* 2000;**97**:1206−11.
30. Bai F, Du W, Liu X, Su L, Li Z, Chen T, et al. A no-responsive ratiometric fluorescent nanoprobe for monitoring drug-induced liver injury in the second near-infrared window. *Anal Chem* 2021;**93**:15279−87.
31. Qiao C, Li D, Liu Y, Zhang S, Liu K, Liu C, et al. Rationalized deep learning super-resolution microscopy for sustained live imaging of rapid subcellular processes. *Nat Biotechnol* 2023;**41**:367−77.
32. Chen H, Fang G, Ren Y, Zou W, Ying K, Yang Z, et al. Super-resolution imaging for in situ monitoring sub-cellular micro-dynamics of small molecule drug. *Acta Pharm Sin B* 2024;**14**:1864−77.
33. Pang Z, Schafroth MA, Ogasawara D, Wang Y, Nudell V, Lal NK, et al. *In situ* identification of cellular drug targets in mammalian tissue. *Cell* 2022;**185**:1793−805.
34. Miao L, Zhou W, Yan C, Zhang Y, Qiao Q, Zhou X, et al. Rapid screening of SARS-Cov-2 inhibitors *via* ratiometric fluorescence of rbd-ace2 complexes in living cells by competitive binding. *Acta Pharm Sin B* 2022;**12**:3739−42.
35. Guo Y, Li D, Zhang S, Yang Y, Liu JJ, Wang X, et al. Visualizing intracellular organelle and cytoskeletal interactions at nanoscale resolution on millisecond timescales. *Cell* 2018;**175**:1430−42.
36. Chen S, Suzuki BM, Dohrmann J, Singh R, Arkin MR, Caffrey CR. A multi-dimensional, time-lapse, high content screening platform applied to schistosomiasis drug discovery. *Commun Biol* 2020;**3**:747.
37. Ntziachristos V. Going deeper than microscopy: the optical imaging frontier in biology. *Nat Methods* 2010;**7**:603−14.
38. Bai J, Wang JT, Mei KC, Al-Jamal WT, Al-Jamal KT. Real-time monitoring of magnetic drug targeting using fibered confocal fluorescence microscopy. *J Control Release* 2016;**244**:240−6.
39. Konig K, Raphael AP, Lin L, Grice JE, Soyer HP, Breunig HG, et al. Applications of multiphoton tomographs and femtosecond laser nanoprocessing microscopes in drug delivery research. *Adv Drug Deliv Rev* 2011;**63**:388−404.
40. Dong Y, Xu T, Yuan L, Wang Y, Yu S, Wang Z, et al. Cerebrospinal fluid efflux through dynamic paracellular pores on venules as a missing piece of the brain drainage system. *Exploration* 2023:20230029.
41. Wu YX, Zhang D, Hu X, Peng R, Li J, Zhang X, et al. Multicolor two-photon nanosystem for multiplexed intracellular imaging and targeted cancer therapy. *Angew Chem Int Ed Engl* 2021;**60**:12569−76.
42. Zong W, Wu R, Chen S, Wu J, Wang H, Zhao Z, et al. Miniature two-photon microscopy for enlarged field-of-view, multi-plane and long-term brain imaging. *Nat Methods* 2021;**18**:46−9.
43. Helmchen F, Denk W. Deep tissue two-photon microscopy. *Nat Methods* 2005;**2**:932−40.
44. Li L, Han Z, Qiu L, Kang D, Zhan Z, Tu H, et al. Label-free multiphoton imaging to assess neoadjuvant therapy responses in breast carcinoma. *Int J Biol Sci* 2020;**16**:1376−87.
45. Chen Y, Kramar EA, Chen LY, Babayan AH, Andres AL, Gall CM, et al. Impairment of synaptic plasticity by the stress mediator crh involves selective destruction of thin dendritic spines *via* rhoa signaling. *Mol Psychiatry* 2013;**18**:485−96.
46. Zhang C, Tabatabaei M, Bélanger S, Girouard H, Moeini M, Lu X, et al. Astrocytic endfoot Ca^{2+} correlates with parenchymal vessel responses during 4-ap induced epilepsy: an *in vivo* two-photon lifetime microscopy study. *J Cereb Blood Flow Metab* 2019;**39**:260−71.
47. Zong W, Obenhaus HA, Skytoen ER, Eneqvist H, de Jong NL, Vale R, et al. Large-scale two-photon calcium imaging in freely moving mice. *Cell* 2022;**185**:1240−56.
48. Watanabe S, Jorgensen EM. Visualizing proteins in electron micrographs at nanometer resolution. *Methods Cell Biol* 2012;**111**:283−306.
49. Gonzalez PM, Nadelson I, Bergner B, Rottmeier S, Thomae AW, Dietzel S. Stimulated emission depletion microscopy with a single depletion laser using five fluorochromes and fluorescence lifetime phasor separation. *Sci Rep* 2022;**12**:14027.
50. Kraus F, Miron E, Demmerle J, Chitiashvili T, Budco A, Alle Q, et al. Quantitative 3D structured illumination microscopy of nuclear structures. *Nat Protoc* 2017;**12**:1011−28.
51. van de Linde S, Loschberger A, Klein T, Heidbreder M, Wolter S, Heilemann M, et al. Direct stochastic optical reconstruction microscopy with standard fluorescent probes. *Nat Protoc* 2011;**6**:991−1009.
52. Calovi S, Soria FN, Tonnesen J. Super-resolution sted microscopy in live brain tissue. *Neurobiol Dis* 2021;**156**:105420.
53. Qiao C, Li D, Guo Y, Liu C, Jiang T, Dai Q, et al. Evaluation and development of deep neural networks for image super-resolution in optical microscopy. *Nat Methods* 2021;**18**:194−202.
54. Villegas-Hernandez LE, Dubey V, Nystad M, Tinguely JC, Coucheron DA, Dullo FT, et al. Chip-based multimodal super-resolution microscopy for histological investigations of cryopreserved tissue sections. *Light Sci Appl* 2022;**11**:43.
55. Chen DY, Sun NH, Lu YP, Hong LJ, Cui TT, Wang CK, et al. Gpr124 facilitates pericyte polarization and migration by regulating the formation of filopodia during ischemic injury. *Theranostics* 2019;**9**:5937−55.
56. Wang L, Chen R, Han G, Liu X, Huang T, Diao J, et al. Super-resolution analyzing spatial organization of lysosomes with an organic fluorescent probe. *Exploration (Beijing)* 2022;**2**:20210215.
57. Hauser M, Wojcik M, Kim D, Mahmoudi M, Li W, Xu K. Correlative super-resolution microscopy: new dimensions and new opportunities. *Chem Rev* 2017;**117**:7428−56.
58. Shi L, Zheng C, Shen Y, Chen Z, Silveira ES, Zhang L, et al. Optical imaging of metabolic dynamics in animals. *Nat Commun* 2018;**9**:2995.
59. Saar BG, Freudiger CW, Reichman J, Stanley CM, Holtom GR, Xie XS. Video-rate molecular imaging *in vivo* with stimulated Raman scattering. *Science* 2010;**330**:1368−70.
60. Campagnola PJ, Loew LM. Second-harmonic imaging microscopy for visualizing biomolecular arrays in cells, tissues and organisms. *Nat Biotechnol* 2003;**21**:1356−60.
61. Chen H, Liu L, Qian K, Liu H, Wang Z, Gao F, et al. Bioinspired large Stokes shift small molecular dyes for biomedical fluorescence imaging. *Sci Adv* 2022;**8**:o3289.
62. Gadella T. New near-infrared fluorescent probes and tools. *Nat Methods* 2022;**19**:654−5.

63. Antaris AL, Chen H, Cheng K, Sun Y, Hong G, Qu C, et al. A small-molecule dye for nir-ii imaging. *Nat Mater* 2016;**15**:235−42.
64. Cai Z, Zhu L, Wang M, Roe AW, Xi W, Qian J. Nir-ii fluorescence microscopic imaging of cortical vasculature in non-human primates. *Theranostics* 2020;**10**:4265−76.
65. Feng Z, Bai S, Qi J, Sun C, Zhang Y, Yu X, et al. Biologically excretable aggregation-induced emission dots for visualizing through the marmosets intravitally: horizons in future clinical nanomedicine. *Adv Mater* 2021;**33**:e2008123.
66. Suo Y, Wu F, Xu P, Shi H, Wang T, Liu H, et al. Nir-ii fluorescence endoscopy for targeted imaging of colorectal cancer. *Adv Healthc Mater* 2019;**8**:e1900974.
67. Zeng X, Liao Y, Qiao X, Liang K, Luo Q, Deng M, et al. Novel nir-ii fluorescent probes for biliary atresia imaging. *Acta Pharm Sin B* 2023;**13**:4578−90.
68. Zhang M, Jin X, Gao M, Zhang Y, Tang BZ. A self-reporting fluorescent salicylaldehyde-chlorambucil conjugate as a type-ii icd inducer for cancer vaccines. *Adv Mater* 2022;**34**:e2205701.
69. Hattori A, Ohta E, Nagai M, Iwabuchi K, Okano H. A new approach to analysis of intracellular proteins and subcellular localization using cellprofiler and imagej in combination. *Methods* 2022;**203**:233−41.
70. Gonzalez JE, Romero I, Barquinero JF, Garcia O. Automatic analysis of silver-stained comets by cellprofiler software. *Mutat Res* 2012;**748**:60−4.
71. Schussele DS, Haller PK, Haas ML, Hunter C, Sporbeck K, Proikas-Cezanne T. Autophagy profiling in single cells with open source cellprofiler-based image analysis. *Autophagy* 2023;**19**:338−51.
72. Chen Q, Shao X, Hao M, Fang H, Guan R, Tian Z, et al. Quantitative analysis of interactive behavior of mitochondria and lysosomes using structured illumination microscopy. *Biomaterials* 2020;**250**:120059.
73. Shao XT, Chen QX, Hu LT, Tian ZQ, Liu LY, Liu F, et al. Super-resolution quantification of nanoscale damage to mitochondria in live cells. *Nano Res* 2020;**13**:2149−55.
74. Chen Q, Shao X, Tian Z, Chen Y, Mondal P, Liu F, et al. Nanoscale monitoring of mitochondria and lysosome interactions for drug screening and discovery. *Nano Res* 2019;**12**:1009−15.
75. Zhang D, Bian Q, Zhou Y, Huang Q, Gao J. The application of label-free imaging technologies in transdermal research for deeper mechanism revealing. *Asian J Pharm Sci* 2021;**16**:265−79.
76. Schindelin J, Arganda-Carreras I, Frise E, Kaynig V, Longair M, Pietzsch T, et al. Fiji: an open-source platform for biological-image analysis. *Nat Methods* 2012;**9**:676−82.
77. Di Z, Klop MJ, Rogkoti VM, Le Devedec SE, van de Water B, Verbeek FJ, et al. Ultra high content image analysis and phenotype profiling of 3D cultured micro-tissues. *Plos One* 2014;**9**:e109688.
78. Liang H, Wang H, Wang S, Francis R, Paxinos G, Huang X. 3D imaging of psd-95 in the mouse brain using the advanced cubic method. *Mol Brain* 2018;**11**:50.
79. Miyazaki T, Chen S, Florinas S, Igarashi K, Matsumoto Y, Yamasoba T, et al. A hoechst reporter enables visualization of drug engagement *in vitro* and *in vivo*: toward safe and effective nanodrug delivery. *Acs Nano* 2022;**16**:12290−304.
80. Bennink LL, Li Y, Kim B, Shin IJ, San BH, Zangari M, et al. Visualizing collagen proteolysis by peptide hybridization: from 3D cell culture to *in vivo* imaging. *Biomaterials* 2018;**183**:67−76.
81. Fang Y, Shang J, Liu D, Shi W, Li X, Ma H. Design, synthesis, and application of a small molecular nir-ii fluorophore with maximal emission beyond 1200 nm. *J Am Chem Soc* 2020;**142**:15271−5.
82. Sturm MB, Joshi BP, Lu S, Piraka C, Khondee S, Elmunzer BJ, et al. Targeted imaging of esophageal neoplasia with a fluorescently labeled peptide: first-in-human results. *Sci Transl Med* 2013;**5**:161r−84r.
83. Thurber GM, Yang KS, Reiner T, Kohler RH, Sorger P, Mitchison T, et al. Single-cell and subcellular pharmacokinetic imaging allows insight into drug action *in vivo*. *Nat Commun* 2013;**4**:1504.
84. Ntziachristos V, Schellenberger EA, Ripoll J, Yessayan D, Graves E, Bogdanov AJ, et al. Visualization of antitumor treatment by means of fluorescence molecular tomography with an annexin v-cy5.5 conjugate. *Proc Natl Acad Sci U S A* 2004;**101**:12294−9.
85. Li C, Zhang Y, Wang M, Zhang Y, Chen G, Li L, et al. *In vivo* real-time visualization of tissue blood flow and angiogenesis using ag2s quantum dots in the nir-ii window. *Biomaterials* 2014;**35**:393−400.
86. Du Y, Xu B, Fu T, Cai M, Li F, Zhang Y, et al. Near-infrared photoluminescent ag2s quantum dots from a single source precursor. *J Am Chem Soc* 2010;**132**:1470−1.
87. Li C, Li F, Zhang Y, Zhang W, Zhang XE, Wang Q. Real-time monitoring surface chemistry-dependent *in vivo* behaviors of protein nanocages *via* encapsulating an nir-ii ag2s quantum dot. *Acs Nano* 2015;**9**:12255−63.
88. Fitzpatrick JA, Andreko SK, Ernst LA, Waggoner AS, Ballou B, Bruchez MP. Long-term persistence and spectral blue shifting of quantum dots *in vivo*. *Nano Lett* 2009;**9**:2736−41.
89. Li Y, Deng Y, Liu J, Fu J, Sun Y, Ouyang R, et al. A near-infrared frequency upconversion probe for nitroreductase detection and hypoxia tumor *in vivo* imaging. *Sensor Actuat B-Chem* 2019;**286**:337−45.
90. Liu Z, Davis C, Cai W, He L, Chen X, Dai H. Circulation and long-term fate of functionalized, biocompatible single-walled carbon nanotubes in mice probed by Raman spectroscopy. *Proc Natl Acad Sci U S A* 2008;**105**:1410−5.
91. Qiu Z, Liu X, Lam J, Tang BZ. The marriage of aggregation-induced emission with polymer science. *Macromol Rapid Commun* 2019;**40**:e1800568.
92. Jiang X, Wang L, Carroll SL, Chen J, Wang MC, Wang J. Challenges and opportunities for small-molecule fluorescent probes in redox biology applications. *Antioxid Redox Signal* 2018;**29**:518−40.
93. Chen G, Cao Y, Tang Y, Yang X, Liu Y, Huang D, et al. Advanced near-infrared light for monitoring and modulating the spatiotemporal dynamics of cell functions in living systems. *Adv Sci (Weinh)* 2020;**7**:1903783.
94. Wang L, Frei MS, Salim A, Johnsson K. Small-molecule fluorescent probes for live-cell super-resolution microscopy. *J Am Chem Soc* 2019;**141**:2770−81.
95. Antaris AL, Chen H, Diao S, Ma Z, Zhang Z, Zhu S, et al. A high quantum yield molecule−protein complex fluorophore for near-infrared ii imaging. *Nat Commun* 2017;**8**:15269.
96. Wu Y, Ali MRK, Chen K, Fang N, El-Sayed MA. Gold nanoparticles in biological optical imaging. *Nano Today* 2019;**24**:120−40.
97. Fan F, Zhang L, Mu F, Shi G. Using a high quantum yield fluorescent probe with two-photon excitation to detect cisplatin in biological systems. *ACS Sens* 2021;**6**:1400−6.
98. Lu G, Nishio N, van den Berg NS, Martin BA, Fakurnejad S, van Keulen S, et al. Co-administered antibody improves penetration of antibody−dye conjugate into human cancers with implications for antibody−drug conjugates. *Nat Commun* 2020;**11**:5667.
99. O'Driscoll LJ, Bryce MR. A review of oligo(arylene ethynylene) derivatives in molecular junctions. *Nanoscale* 2021;**13**:10668−711.
100. Dong P, Stellmacher J, Bouchet LM, Nieke M, Kumar A, Osorio-Blanco ER, et al. A dual fluorescence-spin label probe for visualization and quantification of target molecules in tissue by multiplexed flim-epr spectroscopy. *Angew Chem Int Ed Engl* 2021;**60**:14938−44.
101. Wu D, Cheung S, Daly R, Burke H, Scanlan EM, O'Shea DF. Synthesis and glycoconjugation of an azido-bf2-azadipyrromethene near-infrared fluorochrome. *Eur J Org Chem* 2014;**2014**:6841−5.
102. Aimon P, Knedlík T, Blažková K, Dvořáková P, Březinová A, Kostka L, et al. Identification of protein targets of bioactive small molecules using randomly photomodified probes. *Acs Chem Biol* 2018;**13**:3333−42.
103. Renault K, Fredy JW, Renard PY, Sabot C. Covalent modification of biomolecules through maleimide-based labeling strategies. *Bioconjug Chem* 2018;**29**:2497−513.
104. Sabeti AM, Okuda M, Cyrenne M, Bourge M, Heck MP, Yoshizawa S, et al. Fluorescent aminoglycoside antibiotics and methods for accurately monitoring uptake by bacteria. *Acs Infect Dis* 2020;**6**:1008−17.

105. Curtin NJ, Wang LZ, Yiakouvaki A, Kyle S, Arris CA, Canan-Koch S, et al. Novel poly(adp-ribose) polymerase-1 inhibitor, ag14361, restores sensitivity to temozolomide in mismatch repair-deficient cells. *Clin Cancer Res* 2004;**10**:881−9.
106. Hernandez VS, Lin C, Tran CH, Ikoma N, Aghaamiri S, Ghosh SC, et al. Receptor-targeted fluorescence-guided surgery with low molecular weight agents. *Front Oncol* 2021;**11**:674083.
107. Zhao XB, Ha W, Gao K, Shi YP. Precisely traceable drug delivery of azoreductase-responsive prodrug for colon targeting *via* multimodal imaging. *Anal Chem* 2020;**92**:9039−47.
108. Kwon YD, Oh JM, La MT, Chung HJ, Lee SJ, Chun S, et al. Synthesis and evaluation of multifunctional fluorescent inhibitors with synergistic interaction of prostate-specific membrane antigen and hypoxia for prostate cancer. *Bioconjug Chem* 2019;**30**:90−100.
109. Liu L, Fang H, Chen Q, Chan MH, Ng M, Wang K, et al. Multiple-color platinum complex with super-large Stokes shift for super-resolution imaging of autolysosome escape. *Angew Chem Int Edit* 2020;**59**:8.
110. Yamaguchi H, On J, Morita T, Suzuki T, Okada Y, Ono J, et al. Combination of near-infrared photoimmunotherapy using trastuzumab and small protein mimetic for HER2-positive breast cancer. *Int J Mol Sci* 2021;**22**:12213.
111. Zhou H, Tourkakis G, Shi D, Kim DM, Zhang H, Du T, et al. Cell-free measurements of brightness of fluorescently labeled antibodies. *Sci Rep* 2017;**7**:41819.
112. Sturm MB, Joshi BP, Lu S, Piraka C, Khondee S, Elmunzer BJ, et al. Targeted imaging of esophageal neoplasia with a fluorescently labeled peptide: first-in-human results. *Sci Transl Med* 2013;**5**:161r−84r.
113. Wang L, Zhang Y, Tian J, Li H, Sun X. Conjugation polymer nanobelts: a novel fluorescent sensing platform for nucleic acid detection. *Nucleic Acids Res* 2011;**39**:e37.
114. Xin Q, Ma H, Wang H, Zhang XD. Tracking tumor heterogeneity and progression with near-infrared ii fluorophores. *Exploration (Beijing)* 2023;**3**:20220011.
115. Yuan H, Jiang A, Fang H, Chen Y, Guo Z. Optical properties of natural small molecules and their applications in imaging and nanomedicine. *Adv Drug Deliv Rev* 2021;**179**:113917.
116. Ma Q, Xu S, Zhai Z, Wang K, Liu X, Xiao H, et al. Recent progress of small-molecule ratiometric fluorescent probes for peroxynitrite in biological systems. *Chemistry* 2022;**28**:e202200828.
117. Roy B, Roy TS, Rahaman SA, Das K, Bandyopadhyay S. A minimalist approach for distinguishing individual lanthanide ions using multivariate pattern analysis. *ACS Sens* 2018;**3**:2166−74.
118. Zou X, Himbert S, Dujardin A, Juhasz J, Ros S, Stover H, et al. Curcumin and homotaurine suppress amyloid-beta25-35 aggregation in synthetic brain membranes. *Acs Chem Neurosci* 2021;**12**:1395−405.
119. Jendzelovsky R, Jendzelovska Z, Kucharova B, Fedorocko P. Breast cancer resistance protein is the enemy of hypericin accumulation and toxicity of hypericin-mediated photodynamic therapy. *Biomed Pharmacother* 2019;**109**:2173−81.
120. Kuzma BA, Pence IJ, Greenfield DA, Ho A, Evans CL. Visualizing and quantifying antimicrobial drug distribution in tissue. *Adv Drug Deliv Rev* 2021;**177**:113942.
121. Miao L, Liu W, Qiao Q, Li X, Xu Z. Fluorescent antibiotics for real-time tracking of pathogenic bacteria. *J Pharm Anal* 2020;**10**:444−51.
122. Pommier Y. Topoisomerase i inhibitors: camptothecins and beyond. *Nat Rev Cancer* 2006;**6**:789−802.
123. Liang Z, Sun Y, Duan R, Yang R, Qu L, Zhang K, et al. Low polarity-triggered basic hydrolysis of coumarin as an and logic gate for broad-spectrum cancer diagnosis. *Anal Chem* 2021;**93**:12434−40.
124. Shaik BB, Katari NK, Seboletswe P, Gundla R, Kushwaha ND, Kumar V, et al. Recent literature review on coumarin hybrids as potential anticancer agents. *Anticancer Agents Med Chem* 2023;**23**:142−63.
125. Yadav SK, Rawat G, Pokharia S, Jit S, Mishra H. Excited-state dynamics of quinine sulfate and its di-cation doped in polyvinyl alcohol thin films near silver nanostructure islands. *ACS Omega* 2019;**4**:5509−16.
126. Kotha RR, Luthria DL. Curcumin: biological, pharmaceutical, nutraceutical, and analytical aspects. *Molecules* 2019;**24**:2930.
127. Forkuo AD, Ansah C, Mensah KB, Annan K, Gyan B, Theron A, et al. *In vitro* anti-malarial interaction and gametocytocidal activity of cryptolepine. *Malaria J* 2017;**16**:496.
128. Qing C, Zhang H, Chen A, Lin Y, Shao J. Effects and possible mechanisms of sanguinarineon the competition between *Raphidiopsis raciborskii* (cyanophyta) and *Scenedesmus obliquus* (chlorophyta): a comparative toxicological study. *Ecotox Environ Safe* 2020;**206**:7.
129. Staneva D, Vasileva-Tonkova E, Makki MS, Sobahi TR, Abdsmall Ie CR, Asiri AM, et al. Synthesis, photophysical and antimicrobial activity of new water soluble ammonium quaternary benzanthrone in solution and in polylactide film. *J Photochem Photobiol B* 2015;**143**:44−51.
130. Sun L, Shang H, Wu Y, Xin X. Hypericin-mediated photodynamic therapy enhances gemcitabine-induced capan-2 cell apoptosis *via* inhibiting nadph level. *J Pharm Pharmacol* 2022;**74**:596−604.
131. Li N, Gao XX, Zheng LJ, Huang QH, Zeng F, Chen HB, et al. Advances in fucoxanthin chemistry and management of neurodegenerative diseases. *Phytomedicine* 2022;**105**:154352.
132. Sugawara T, Ganesan P, Li ZS, Manabe Y, Hirata T. Siphonaxanthin, a green algal carotenoid, as a novel functional compound. *Mar Drugs* 2014;**12**:3660−8.
133. Sun Y, Sun P, Li Z, Qu L, Guo W. Natural flavylium-inspired far-red to nir-ii dyes and their applications as fluorescent probes for biomedical sensing. *Chem Soc Rev* 2022;**51**:7170−205.
134. Wei Y, Kong L, Chen H, Liu Y, Xu Y, Wang H, et al. Super-resolution image-based tracking of drug distribution in mitochondria of a label-free naturally derived drug molecules. *Chem Eng J* 2022;**429**:132134.
135. Denisov SS, Kotova EA, Plotnikov EY, Tikhonov AA, Zorov DB, Korshunova GA, et al. A mitochondria-targeted protonophoric uncoupler derived from fluorescein. *Chem Commun (Camb)* 2014;**50**:15366−9.
136. Zhang HW, Lv C, Zhang LJ, Guo X, Shen YW, Nagle DG, et al. Application of omics- and multi-omics-based techniques for natural product target discovery. *Biomed Pharmacother* 2021;**141**:111833.
137. O'Hagan S, Kell DB. Structural similarities between some common fluorophores used in biology, marketed drugs, endogenous metabolites, and natural products. *Mar Drugs* 2020;**18**:582.
138. Garcia-Plazaola JI, Fernandez-Marin B, Duke SO, Hernandez A, Lopez-Arbeloa F, Becerril JM. Autofluorescence: biological functions and technical applications. *Plant Sci* 2015;**236**:136−45.
139. Henrich CJ, Beutler JA. Matching the power of high throughput screening to the chemical diversity of natural products. *Nat Prod Rep* 2013;**30**:1284−98.
140. Crampon K, Giorkallos A, Deldossi M, Baud S, Steffenel LA. Machine-learning methods for ligand−protein molecular docking. *Drug Discov Today* 2022;**27**:151−64.
141. Maynard JA, Lindquist NC, Sutherland JN, Lesuffleur A, Warrington AE, Rodriguez M, et al. Surface plasmon resonance for high-throughput ligand screening of membrane-bound proteins. *Biotechnol J* 2009;**4**:1542−58.
142. Huang L, Zhang C. Microscale thermophoresis (mst) to detect the interaction between purified protein and small molecule. *Methods Mol Biol* 2021;**2213**:187−93.
143. Kokubo S, Ohnuma S, Murakami M, Kikuchi H, Funayama S, Suzuki H, et al. A phenylfuro coumarin derivative reverses abcg2-mediated multidrug resistance *in vitro* and *in vivo*. *Int J Mol Sci* 2021;**22**:12502.
144. Scholz AK, Klebl BM, Morkel M, Lehrach H, Dahl A, Lange BM. A flexible multiwell format for immunofluorescence screening microscopy of small-molecule inhibitors. *Assay Drug Dev Technol* 2010;**8**:571−80.

145. Zhang JF, Liu B, Hong I, Mo A, Roth RH, Tenner B, et al. An ultrasensitive biosensor for high-resolution kinase activity imaging in awake mice. *Nat Chem Biol* 2021;**17**:39−46.
146. Yun SW, Kang NY, Park SJ, Ha HH, Kim YK, Lee JS, et al. Diversity oriented fluorescence library approach (dofla) for live cell imaging probe development. *Acc Chem Res* 2014;**47**:1277−86.
147. Lee JS, Kang NY, Kim YK, Samanta A, Feng S, Kim HK, et al. Synthesis of a bodipy library and its application to the development of live cell glucagon imaging probe. *J Am Chem Soc* 2009;**131**:10077−82.
148. Lee JS, Kim HK, Feng S, Vendrell M, Chang YT. Accelerating fluorescent sensor discovery: unbiased screening of a diversity-oriented bodipy library. *Chem Commun (Camb)* 2011;**47**:2339−41.
149. Zhu L, Shan L, Zhu J, Li L, Li S, Wang L, et al. Discovery of a natural fluorescent probe targeting the plasmodium falciparum cysteine protease falcipain-2. *Sci China Life Sci* 2020;**63**:1016−25.
150. Gao M, Lee SH, Das RK, Kwon HY, Kim HS, Chang YT. A slc35c2 transporter-targeting fluorescent probe for the selective detection of b lymphocytes identified by slc-crispri and unbiased fluorescence library screening. *Angew Chem Int Ed Engl* 2022;**61**:e202202095.
151. Kuriki Y, Yoshioka T, Kamiya M, Komatsu T, Takamaru H, Fujita K, et al. Development of a fluorescent probe library enabling efficient screening of tumour-imaging probes based on discovery of biomarker enzymatic activities. *Chem Sci* 2022;**13**:4474−81.
152. Zheng Q, Zhu Y, Wang A, Yang P, Wang X, Shuai W, et al. Structure-based virtual screening for novel p38 mapk inhibitors and a biological evaluation. *Acta Materia Medica* 2023;**2**:377−85.
153. Fischer T, Gazzola S, Riedl R. Approaching target selectivity by de novo drug design. *Expert Opin Drug Discov* 2019;**14**:791−803.
154. Lim S, Haque MM, Su D, Kim D, Lee JS, Chang YT, et al. Development of a bodily-based fluorescent probe for imaging pathological tau aggregates in live cells. *Chem Commun (Camb)* 2017;**53**:1607−10.
155. Zheng Z, Zhang T, Liu H, Chen Y, Kwok R, Ma C, et al. Bright near-infrared aggregation-induced emission luminogens with strong two-photon absorption, excellent organelle specificity, and efficient photodynamic therapy potential. *Acs Nano* 2018;**12**:8145−59.
156. Zeng C, Tan Y, Sun L, Long Y, Zeng F, Wu S. Renal-clearable probe with water solubility and photostability for biomarker-activatable detection of acute kidney injuries *via* nir-ii fluorescence and optoacoustic imaging. *ACS Appl Mater Interfaces* 2023;**15**:17664−74.
157. Zhang L, Jiang FL, Liu Y, Jiang P. Mitochondrial targeting long-term near-infrared imaging and photodynamic therapy aggregation-induced emission luminogens manipulated by thiophene. *J Phys Chem Lett* 2022;**13**:3462−9.
158. Li B, Liu H, He Y, Zhao M, Ge C, Younis MR, et al. A "self-checking" pH/viscosity-activatable nir-ii molecule for real-time evaluation of photothermal therapy efficacy. *Angew Chem Int Edit* 2022;**61**:8.
159. Vinegoni C, Feruglio PF, Gryczynski I, Mazitschek R, Weissleder R. Fluorescence anisotropy imaging in drug discovery. *Adv Drug Deliv Rev* 2019;**151**−**152**:262−88.
160. Wu P, Liu X, Duan Y, Pan L, Sun Z, Chu H, et al. Znpc photosensitizer-loaded peony-shaped fese2 remotely controlled by near-infrared light for antimycobacterial therapy. *Acta Materia Medica* 2023;**2**:260−9.
161. Chen SX, Zhang DY, Seelig G. Conditionally fluorescent molecular probes for detecting single base changes in double-stranded dna. *Nat Chem* 2013;**5**:782−9.
162. Wu X, Wang R, Kwon N, Ma H, Yoon J. Activatable fluorescent probes for *in situ* imaging of enzymes. *Chem Soc Rev* 2022;**51**:450−63.
163. Zhou Y, Zhang Y, Lian X, Li F, Wang C, Zhu F, et al. Therapeutic target database update 2022: facilitating drug discovery with enriched comparative data of targeted agents. *Nucleic Acids Res* 2022;**50**:D1398−407.
164. Liu DS, Tangpeerachaikul A, Selvaraj R, Taylor MT, Fox JM, Ting AY. Diels−Alder cycloaddition for fluorophore targeting to specific proteins inside living cells. *J Am Chem Soc* 2012;**134**:792−5.
165. Glymenaki E, Kandyli M, Apostolidou CP, Kokotidou C, Charalambidis G, Nikoloudakis E, et al. Design and synthesis of porphyrin-nitrilotriacetic acid dyads with potential applications in peptide labeling through metallochelate coupling. *ACS Omega* 2022;**7**:1803−18.
166. Zhang L, Yan Z, Wang Y, Song C, Miao G. Design, synthesis, and biological application of novel photoaffinity probes of dihydropyridine derivatives, bay r3401. *Molecules* 2019;**24**:2394.
167. Bai Q, Yang C, Yang M, Pei Z, Zhou X, Liu J, et al. Ph-dominated selective imaging of lipid droplets and mitochondria *via* a polarity-reversible ratiometric fluorescent probe. *Anal Chem* 2022;**94**:2901−11.